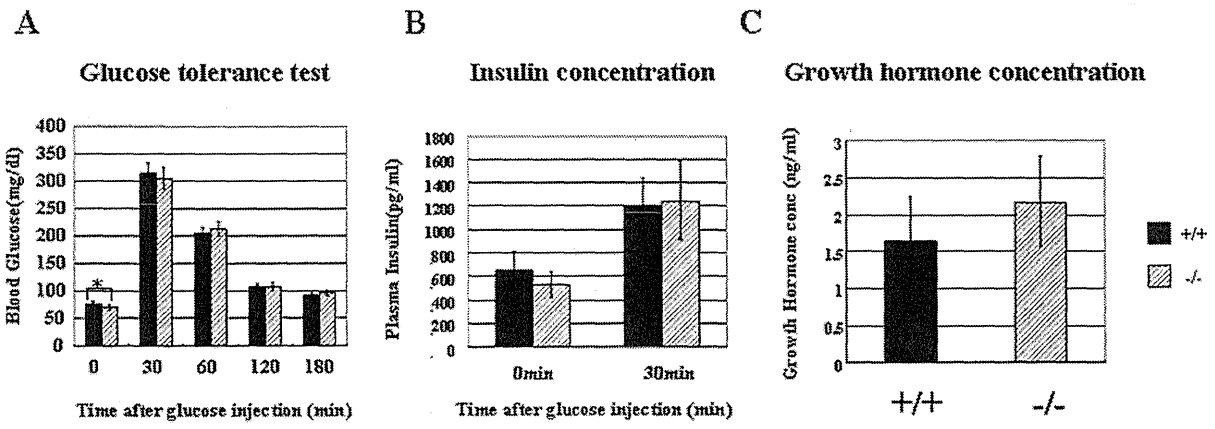

Figure 9. Glucose metabolism and growth hormone levels in wild-type and *Dicer1*-hypomorphic mice. A: Glucose tolerance test. Fasted 8-week-old mice received an intraperitoneal injection of glucose (2 mg/g body weight). B: Insulin concentration. Plasma insulin was measured before and after the intraperitoneal glucose injection. C: Growth hormone concentration. Plasma growth hormone concentrations were measured in wild-type and *Dicer1*-hypomorphic mice. A, B: Values are expressed as the means±S.D. (n = 10 per group). C: Values are expressed as the means±S.D. (n = 10 per group).*, $P<0.05$.
doi:10.1371/journal.pone.0004212.g009

C57BL/6 mice. *Dicer1* heterozygous mice were backcrossed with C57BL/6 mice for 12 generations. All animal experiments were approved by the Animal Research Ethics Board at the Gunma University.

Histochemistry and immunohistochemistry

Tissues and embryos were fixed overnight in formalin at 4°C and embedded in paraffin. Standard techniques were used for the embedding, sectioning and staining of tissues. Sections were cut at 5 μm. Immunohistochemistry was performed as follows: The slides were dewaxed and washed in PBS, and blocked in 1% BSA for 30 min. They were then incubated with primary antibodies overnight at 4°C in PBS containing 1% BSA, washed in PBS, and incubated with the appropriate secondary antibodies for 1 hour at room temperature. The slides were washed in PBS and mounted with Pristine Mount (Parma) with DAPI. The primary antibodies used were rabbit anti-glucagon (1:200, DAKO) and guinea pig anti-insulin (1:200, DAKO), rabbit Ki67 monoclonal antibody (Lab Vision), and Pdx1 (a gift from Christopher V. Wright (Vanderbilt University, Nashville)). The secondary antibodies were conjugated to rodamin (1:200, Jackson) and Alexa 488 (1:200, Molecular Probes). The slides were examined with a Nikon ECLIPSC TE300 and images were obtained with a LEICA DFC400 camera.

Measurement of islet area

ß-cell mass was measured using Image J software (NIH). Islet numbers and areas were averaged from 6 animals, with six sections from each animal, 250 μm apart.

RNA extraction and quantitative RT-PCR

Total RNA was prepared from isolated tissues using the RNeasy mini kit (Qiagen) with a modified protocol to purify total RNA containing miRNA from animal tissues. Differential gene expression was confirmed using the SYBR Premix Ex Taq (TAKARA) in accord with the manufacturer's instructions. The reaction was performed using the SYBER Green program on an ABI PRISM 7700 sequence detector system (Applied Biosystems). The expression of mRNA was normalized to that of GAPDH mRNA.

Primer sequences were as follows, ActRIIA: 5′-AGCGGAG-CTGACAGTGATTT-3′, 5′-CATACACGCACAACACACCA-3′ ActRIIB: 5′-TGGACATCCATGAGGTGAGA-3′, 5′-CAGCAG-CTGTAGTGGCTTCA-3′

miRNA microarray

Small RNAs were labeled with a miRNA labeling Reagent & Hybridization Kit (Agilent) based on the manufacturer's instructions. The Cy3-labeled RNA molecules were hybridized with a Mouse miRNA microarray (Agilent), consisting of control probes, mismatch probes, and 567 capture probes as registered and annotated in Sanger miRBase v10.1. A DNA MicroArray Scanner (Agilent) was used to scan images. The scanned images were analyzed with Agilent Feature Extractin Ver.9.5.3 (Agilent). Data were normalized globally per array. The net intensity values were normalized to per-chip median values.

Glucose tolerance test and insulin concentration

After overnight fasting, 2 mg/g (body weight) of glucose was administered intraperitoneally. Blood samples were drawn intraperitoneally from the tail at different times, and the blood glucose concentration was measured with an automatic blood glucose meter, Freestyle Freedom (NIPRO). Whole blood was collected and centrifuged, and the plasma was stored at −80°C. The insulin concentration was measured with an insulin measurement kit (Morinaga) in accordance with the manufacturer's instructions.

Growth hormone measurements

Growth hormone concentrations of wild-type and *Dicer1*-hypomorphic mice were measured with a rat/mouse growth hormone ELISA kit (LINCO Research).

Data analysis

Data were analyzed by the one-sample t-test and independent samples t-test. Data are the means±S.D.

Acknowledgments

We thank the Mutant Mouse Regional Resource Center (MMRRC) for providing RRF266 cells.

Author Contributions

Conceived and designed the experiments: SM IH. Performed the experiments: SM AH TH MK TK KN RM. Analyzed the data: SM IK TK TO KM. Contributed reagents/materials/analysis tools: SM. Wrote the paper: SM.

References

1. Gregory RI, Yan KP, Amuthan G, Chendrimada T, Doratotaij B, et al. (2004) The microprocessor complex mediates the genesis of microRNAs. Nature 432: 235–240.
2. Bernstein E, Caudy AA, Hammond SM, Hannon GJ (2001) Role for a bidentate ribonuclease in the initiation step of RNA interference. Nature 409: 363–366.
3. Hammond SM, Boettcher S, Caudy AA, Kobayashi R, Hannon GJ (2001) Argonaute2, a link between genetic and biochemical analyses of RNAi. Science 293: 1146–1150.
4. Lagos-Quintana M, Rauhut R, Yalcin A, Meyer J, Lendeckel W, Tuschl T (2002) Identification of microRNA from mouse. Current Biology 12: 735–739.
5. Wienholds E, Kloosterman WP, Misaka E, Alvarez-Saavedra E, Berezikov E, et al. (2005) MicroRNA expression in zebrafish embryonic development. Science 309: 310–311.
6. Bernstein E, Kim SY, Carmell MA, Murchison EP, Alcorn H, et al. (2003) Dicer is essential for mouse development. Nat Genet 35: 215–217.
7. Yang WY, Yang DD, Songqing N, Sandusky GE, Zhang Q, et al. (2005) Dicer is required for embryonic angiogenesis during mouse development. J Biol Chem 280: 9330–9335.
8. Harfe BD, McManus MT, Mansfield JH, Hornstein E, Tabin CJ (2005) The RNaseIII enzyme Dicer is required for morphogenesis but not patterning of the vertebrate limb. Proc Natl Acad Sci USA 102: 10898–10903.
9. Harris KS, Zhang Z, McManus MT, Harfe BD, Sun X (2006) Dicer function is essesntial for lung epithelium morphogenesis. Proc Natl Acad Sci USA 103: 2208–2213.
10. Andl T, Murchison EP, Liu F, Zhang Y, Yunta-Gonzalez M, et al. (2006) The miRNA-processing enzyme Dicer is essential for morphogenesis and maintenance of hair follicles. Current Biology 16: 1041–1046.
11. Lynn FC, Skewes-Cox BAP, Kosaka Y, McManus MT, Harfe BD, et al. (2007) MicroRNA expression is required for pancreatic islet cell genesis in the mouse. Diabetes 56: 2938–2945.
12. Cobb BS, Nesterova TB, Thompson E, Hertweck A, O'Connor E, et al. (2005) T cell lineage choice and differentiation in the absence of the RNase III enzyme Dicer. J Exp Med 20: 1367–1373.
13. Fukasawa M, Morita S, Kimura M, Horii T, Ochiya T, et al. (2006) Genomic imprinting in Dicer1-hypomorphic mice. Cytogenet Genome Res 113: 138–143.
14. Habener JF, Kemp DM, Thomas MK (2005) Minireview: Transcriptional regulation in pancreatic development. Endocrinology 146: 1025–1034.
15. Ackermann AM, Gannon M (2007) Molecular regulation of pancreatic β-cell mass development, maintenance, and expansion. J Mol Endo 38: 193–206.
16. Dor Y, Brown J, Martinez OI, Melton DA (2004) Adult pancreatic beta-cells are formed by self-duplication rather than stem-cell differentiation. Nature 429: 41–46.
17. Teta M, Rankin MM, Long SY, Stein GM, Kushner JA (2007) Growth and regeneration of adult β cells dose not involve specialized progenitors. Dev Cell 12: 817–829.
18. Bonner-Weir S, Baxter LA, Schuppin GT, Smith FE (1993) A second pathway for regenerating of adult exocrine and endocrine pancreas. A possible recapitulation of embryonic development. Diabetes 42: 1715–1720.
19. Bertelli E, Bendayan M (1997) Intermediate endocrine-acinar pancreatic cells in duct ligation conditions. Am J Physiol Cell Physiol 273: C1641–C1649.
20. Bonner-Weir S, Toschi E, Inada A, Reits P, Fonseca SY, et al. (2004) The pancreatic ductal epithelium serves as apotential pool of progenitor cells. Pediatric Diabetes 5: 16–22.
21. Xu X, D'Hoker J, Stange G, Bonne S, De Leu N, et al. (2008) β cells can be generated from endogenous progenitors in injured adult mouse pancreas. Cell 132: 197–207.
22. Kritzik MR, Jones E, Chen Z, Krakowski M, Krahl T, et al. (1999) Pdx-1 and Msx-2 expression in the regenerating and developing pancreas. J Endocrinol 163: 523–530.
23. Song SY, Gannon M, Wahington MK, Scoggins CR, Meszoely IM, et al. (1999) Pdx-1 expressing pancreatic epithelium and islet neogenesis in transgenic mice overexpressing transforming growth factor alpha. Gastroenterology 117: 1416–1426.
24. Shiozaki S, Tajima T, Zhang YQ, Furukawa M, Nakazato Y, et al. (1999) Impaired differentiation of endocrine cells of pancreas in transgenic mouse expressing the truncated type II activin receptor. Biochimica et Biophysica Acta 1450: 1–11.
25. Attisano L, Wrana JL, Cheifetz S, Massague J (1992) Novel activin receptors: dinsinct genes and alternative mRNA splicing generate a repertoire of serine/threonine kinase receptors. Cell 68: 97–108.
26. Mathews LS (1994) Activin receptors and cellular signaling by the receptor serine kinase family. Endocr Rev 15: 310–325.
27. Attisano L, Carcamo J, Ventura F, Weis FM, Massague J, et al. (1993) Identificatin of human activin and TGF beta type I receptors that form heteromeric kinase complexes with type II receptors. Cell 75: 671–680.
28. Yamashita H, Ten Dijke P, Huylebroeck D, Sampath TK, Andries M, et al. (1995) Osteogenic protein-1 binds to activin type II receptors and induce certain activin-like effectors. J Cell Biol 130: 217–226.
29. Lee SJ, McPherron AC (2001) Regulation of myostain activity and muscle growth. Proc Natl Acad Sci USA 98: 9306–9311.
30. Yeo C, Whitman M (2001) Nodal signals to Smads through Cripto-dependent and Cripto-independent mechanisms. Mol Cell 7: 949–957.
31. Oh SP, Yeo CY, Lee Y, Schrewe H, Whitman M, et al. (2002) Activin type IIA and type IIB receptors mediate Gdf11 signaling in axial vertebral patterning. Gene Dev 16: 2749–2754.
32. Gittes GK, Rutter WJ (1992) Onset of cell-specific gene expression in the developing mouse pancreas. Proc Natl Acad Sci USA 89: 1128–1132.
33. Teitelman G, Alpert S, Polak JM, Martinez A, Hanahan D (1993) Precursor cells of mouse endocrine pancreas coexpress insulin, glucagon and the neuronal proteins tyrosine hydroxylase and neuropeptide Y, but not pancreatic polypeptide. Development 118: 1031–1039.
34. Stryke D, Kawamoto M, Huang CC, Johns SJ, King LA (2003) BayGenomics: a resorce of insertional mutations in mouse embryonic stem cells. Nucleic Acids Res 31: 278–281.

STEM CELLS®

TISSUE-SPECIFIC STEM CELLS

Roundabout 4 Is Expressed on Hematopoietic Stem Cells and Potentially Involved in the Niche-Mediated Regulation of the Side Population Phenotype

FUMI SHIBATA,[a] YUKO GOTO-KOSHINO,[a] YOSHIHIRO MORIKAWA,[b] TADASUKE KOMORI,[b] MIYUKI ITO,[c] YUMI FUKUCHI,[c] JEFFREY P. HOUCHINS,[d] MONICA TSANG,[d] DEAN Y. LI,[e,f] TOSHIO KITAMURA,[a] HIDEAKI NAKAJIMA[c]

[a]Division of Cellular Therapy, Advanced Clinical Research Center, and [c]Center of Excellence, Institute of Medical Science, University of Tokyo, Tokyo, Japan; [b]Department of Anatomy and Neurobiology, Wakayama Medical College, Wakayama, Japan; [d]R&D Systems Inc., Minneapolis, Minnesota, USA; Departments of [e]Oncological Sciences and [f]Medicine, University of Utah, Salt Lake City, Utah, USA

Key Words. Hematopoietic stem cell • Robo • Roundabout • Slit • Surface marker

ABSTRACT

Roundabout (Robo) family proteins are immunoglobulin-type cell surface receptors that are expressed predominantly in the nervous system. The fourth member of this family, Robo4, is distinct from the other family members in that it is expressed specifically in endothelial cells. In this study, we examined the expression of Robo4 in hematopoietic stem cells (HSCs) and its possible role in HSC regulation. Robo4 mRNA was specifically expressed in murine HSCs and the immature progenitor cell fraction but not in lineage-positive cells or differentiated progenitors. Moreover, flow cytometry showed a correlation between higher expression of Robo4 and immature phenotypes of hematopoietic cells. Robo4^{high} hematopoietic stem/progenitor cells presented higher clonogenic activity or long-term repopulating activity by colony assays or transplantation assays, respectively. A ligand for Robo4, Slit2, is specifically expressed in bone marrow stromal cells, and its expression was induced in osteoblasts in response to myelosuppressive stress. Interestingly, overexpression of Robo4 or Slit2 in HSCs resulted in their decreased residence in the c-Kit$^+$Sca-1$^+$Lineage$^-$-side population fraction. These results indicate that Robo4 is expressed in HSCs, and Robo4/Slit2 signaling may play a role in HSC homeostasis in the bone marrow niche. STEM CELLS *2009;27:183–190*

Disclosure of potential conflicts of interest is found at the end of this article.

INTRODUCTION

Roundabout (Robo) family proteins are immunoglobulin-type cell surface receptors that are expressed predominantly in the nervous system [1]. Slit, a ligand for Robo, is a large secreted protein that is also expressed in brain [1]. The Robo family comprises four family members, Robo1–Robo4, and the Slit family consists of three family members, Slit1–Slit3. Robo and Slit were first described in *Drosophila* as critical molecules in axon path finding and migration of neuronal cells [2]. In mammals, Slit/Robo signaling acts as a repulsive axon guidance cue for developing neurons and inhibits neuronal migration, thus playing a critical role for correct wiring of the neuronal network [3]. In the hematopoietic system, Slit2 has been shown to inhibit chemotactic migration of lymphocytes induced by SDF-1 [4]. In addition, Slit2/Robo1 signaling plays a critical role in tumor angiogenesis [5]. Robo4 was first identified by in silico database mining as a homolog of Robo1 [6, 7]. Robo4 is unique in its expression pattern that is specific to endothelial cells, whereas it shows functional similarity to other Robo family members, such as a binding with Slit2 or an inhibitory effect for cellular migration [7]. In hematopoiesis, Forsberg et al. have reported an extensive transcriptome analysis of long-term (LT)-hematopoietic stem cells (HSCs), short-term (ST)-HSCs, and multipotent progenitors (MPPs) and showed that Robo4 is one of the differentially expressed genes among these three primitive hematopoietic cell populations [8]. However, differential expression of Robo4 in whole hematopoietic system has not been examined.

HSCs are a rare population of cells that can support life-long hematopoiesis. They are characterized by their unique capacity to self-renew and differentiate into all blood cell lineages. HSCs reside in the specific microenvironment known as the niche in the adult bone marrow (BM). The niche is thought to be located on the surface of trabecular bones, and osteoblasts lining the surface of these bones are reported to be one of the critical niche components [9, 10]. Side population (SP) phenotype, identified by as the activity of Hoechst 33342 dye efflux, is one of the hallmarks of

Author contributions: F.S., Y.G.-K., Y.M., T.K., M.I., and Y.F.: Collection and assembly of data; J.P.H., M.T., and D.Y.L.: provision of study material; T.K.: administrative support; H.N.: conception and design, financial support, data analysis and interpretation, manuscript writing, final approval of manuscript. F.S. and Y.G.-K. contributed equally to this work.

Correspondence: Hideaki Nakajima, M.D., Ph.D., Division of Hematology, Department of Internal Medicine, Keio University School of Medicine, 35 Shinanomachi, Shinjuku-ku, Tokyo 160-8582, Japan. Telephone: 81-3-5363-3785; Fax: 81-3-3353-3515; e-mail: hnakajim@sc.itc.keio.ac.jp Received April 4, 2008; accepted for publication September 30, 2008; first published online in STEM CELLS *EXPRESS* October 16, 2008. 1066-5099/2008/$30.00/0 doi: 10.1634/stemcells.2008-0292

quiescent HSCs in the BM niche [11, 12]. It has been shown that many of the quiescent HSCs reside in the c-Kit$^+$Sca-1$^+$Lineage$^-$ (KSL)-SP, and angiopoietin-1/Tie-2 signaling induces HSC quiescence and increases cells in the KSL-SP [13]. Moreover, quiescent HSCs move from the SP to a main population (MP) of non-SP cells when they are recruited into the cell cycle upon myelosuppressive stimuli, such as 5-fluorouracil (5-FU) treatment. However, the molecular mechanism regulating this transition remains unclear.

In a search for novel surface molecules expressed on HSCs, we found that Robo4 was highly expressed in the HSCs and the immature progenitor cell fraction. Moreover, Slit2 was specifically expressed in bone marrow stromal cells, and interestingly, the expression was induced in osteoblasts in response to myelosuppressive stimuli, such as 5-FU treatment. Surprisingly, enhanced Slit2/Robo4 signaling in HSCs resulted in the shift of their residence from SP to non-SP. These results suggest a possible involvement of Slit2/Robo4 signaling in the regulation of HSC homeostasis by the BM niche.

Materials and Methods

Cells and Mice

MS10, PA6, and OP9 cells [14, 15] were cultured as previously described [16]. Primary BM stromal cells were obtained by culturing the adherent fraction of whole BM cells from B6 mice in α-minimal essential medium/10% fetal bovine serum on the culture dish and expanding them for 2 weeks.

RNA Extraction and Reverse Transcription-Polymerase Chain Reaction

Messenger RNA (mRNA) was isolated using a Micro-FastTrack 2.0 mRNA Isolation Kit (Invitrogen, Carlsbad, CA, http://www.invitrogen.com) according to the manufacturer's protocol. First-strand cDNA was synthesized with SuperScript II reverse transcriptase (Invitrogen). The quantity of cDNA was normalized according to the expression of glyceraldehyde-3-phosphate dehydrogenase measured by real-time reverse transcription (RT)-polymerase chain reaction (PCR) using a Light Cycler Fast Start DNA SYBR Green I kit (Roche Diagnostics, Basel, Switzerland, http://www.roche-applied-science.com). Semiquantitative RT-PCR was performed using Ex Taq-HS polymerase (Takara Bio, Shiga, Japan, http://www.takara-bio.com). The sequences of primers used for RT-PCR are shown in supporting information Table 1.

Antibodies

Anti-mouse c-Kit-allophycocyanin (APC) (2B8), Sca-1-fluorescein isothiocyanate (FITC) (D7), Sca-1-APC (D7), and CD34-FITC (RAM34) antibodies were from BD Pharmingen (San Diego, http://www.bdbiosciences.com/index_us.shtml). Anti-mouse c-Kit-phycoerythrin (PE)-Cy7 (2B8) was from BioLegend (San Diego, http://www.biolegend.com). Anti-mouse Robo4 monoclonal antibodies were raised against the extracellular domain of Robo4 by immunizing rats with Y3Ag1.2.3 cells expressing mouse Robo4. The purified antibodies were labeled with PE using PhycoLink R-Phycoerythrin Conjugation Kit (PROzyme, San Leandro, CA, http://www.prozyme.com).

Flow Cytometry

BM cells were obtained by flushing out femurs and tibias from 8–12-week-old mice with phosphate-buffered saline (PBS). Depletion of lineage-positive cells and staining and fluorescence-activated cell sorting (FACS) of KSL and CD34$^-$KSL cells were described previously [17]. Stained cells were analyzed by FACSAria or FACSVantage (Becton, Dickinson and Company, Franklin Lakes, NJ, http://www.bd.com). Hoechst staining of lineage depleted cells was performed with 5 μg/ml Hoechst 33342 (Sigma-Aldrich, St. Louis, http://www.sigmaaldrich.com) at 37°C for 90 minutes as previously described by Goodell et al. [11].

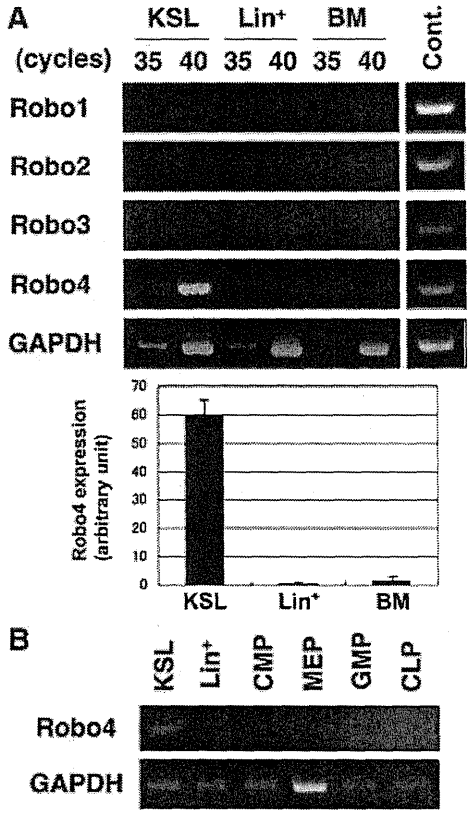

Figure 1. Expression of Robo4 in primitive hematopoietic cells. **(A):** Expression of Robo family genes. KSL and Lin$^+$ cells were sorted by flow cytometry and subjected to RNA extraction. Upper panel: the expressions of the Robo1–Robo4 genes were examined by reverse transcription (RT)-polymerase chain reaction (PCR). The GAPDH gene was examined as a cont. Brain cDNA was used as a positive cont. Lower panel: quantitative RT-PCR for the Robo4 gene (mean ± SD; $n = 3$). **(B):** The expression of the Robo4 gene in various hematopoietic progenitors was examined by RT-PCR. Abbreviations: BM, bone marrow; CLP, common lymphoid progenitor; CMP, common myeloid progenitor; Cont., control; GAPDH, glyceraldehyde-3-phosphate dehydrogenase; GMP, granulocyte/monocyte progenitor; KSL, c-Kit$^+$Sca-1$^+$Lineage$^-$; Lin, lineage marker; MEP, megakaryocyte/erythroid progenitor; Robo, roundabout.

Retrovirus Production, Infection, and Bone Marrow Transplantation

Retrovirus was produced as previously described [16]. Briefly, retrovirus plasmids [18] were transiently transfected into PLAT-E [19] cells using Fugene (Roche Diagnostics), and retrovirus supernatant was collected after 48 hours of transfection. Infection of BM cells with retrovirus was carried out using Retronectin (Takara Bio) according to the manufacturer's protocol. Bone marrow transplantation of infected cells was performed as previously described [16] using B6-Ly5.1 mice (Sankyo Lab Service Co., Tokyo, http://www.sankyolabo.co.jp) as donors and B6-Ly5.2 mice (CLEA Japan, Tokyo, http://www.clea-japan.com) as recipients and competitors. For competitive repopulation assay of Robo4$^+$KSL or Robo4$^-$KSL cells, 100 cells for each group were sorted from BM mononuclear cells of B6-Ly5.1 mice and transplanted with 2×10^5 competitor cells (whole BM cells from Ly5.2 mice) into lethally irradiated (950R) recipient mice (B6-Ly5.2). Eight- to 12-week-old mice were used in all experiments. All animal experiments were reviewed and approved by the institutional review board of the Institute of Medical Science, University of Tokyo.

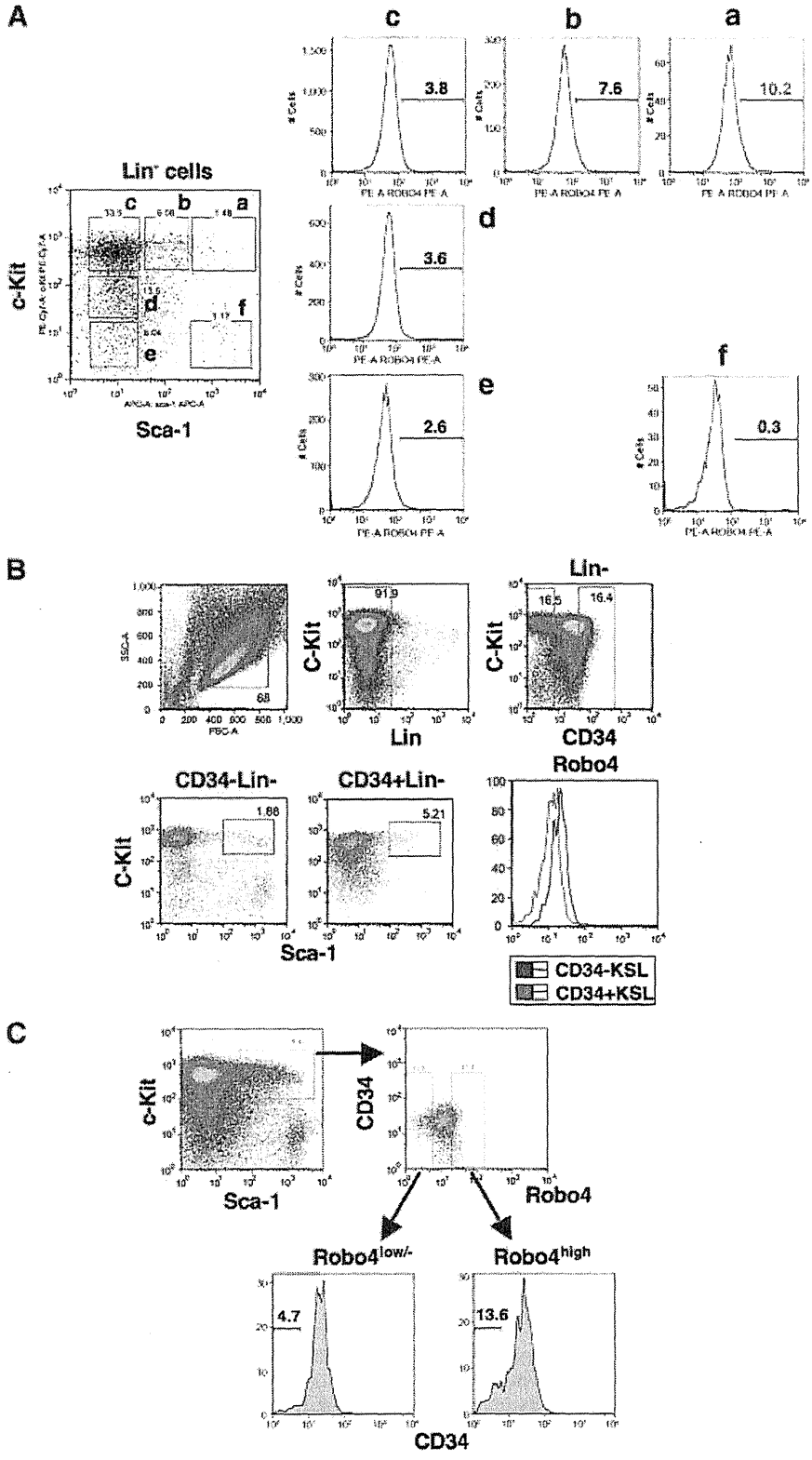

Figure 2. Expression of Robo4 by flow cytometry. **(A):** Lineage-depleted murine bone marrow cells were stained with Sca-1-fluorescein isothiocyanate (FITC), c-Kit-APC, and Robo4-PE. Cells were fractionated according to the expression of c-Kit and Sca-1 into six populations **(Aa–Af)**, and the expression of Robo4 in each fraction was analyzed. **(B):** Robo4 is highly expressed in $CD34^{-}$KSL cells. $CD34^{-}$KSL and $CD34^{+}$KSL cells were gated as shown in the figure and examined for Robo4. **(C):** $Robo4^{high}$KSL cells contain more $CD34^{-}$ cells. $Robo4^{high}$KSL or $Robo4^{low/-}$KSL cells were gated as shown and examined for CD34 expression. Abbreviations: FSC, forward scatter; KSL, $c\text{-}Kit^{+}Sca\text{-}1^{+}Lineage^{-}$; Lin, lineage marker; PE, phycoerythrin; Robo, roundabout; SSC, side scatter.

Colony-Forming Cell Assay

For the colony-forming cell assay, cells were sorted by FACS and deposited into MethoCult GF M3434 (StemCell Technologies, Vancouver, BC, Canada, http://www.stemcell.com). The number and type of colonies were assessed at day 7 of culture.

Immunostaining

Mice treated with 5-FU (150 mg/kg, i.p.) for 3 days were fixed by perfusing them with Zamboni's fixative. Femurs were then dissected and decalcified in 10% EDTA at 4°C. The bones were embedded in Tissue-Tek OCT Compound (Sakura Finetek, Tor-

rance, CA, http://www.sakura.com), frozen, and sectioned in 5-μm-thick slices using a cryostat (Leica, Heerbrugg, Switzerland, http://www.leica.com). Sections were blocked with biotin and normal donkey serum and stained with anti-Slit2 (G-19; Santa Cruz Biotechnology Inc., Santa Cruz, CA, http://www.scbt.com) and anti-osteopontin (Takara Bio) antibodies, which were then subjected to secondary staining with anti-goat IgG-biotin and anti-mouse IgG-Cy3 and tertiary staining with streptoavidin-Cy2. Sections were washed three times for 5 minutes in PBS between steps and finally mounted in Vectashield anti-fading medium (Vector Laboratories, Burlingame, CA, http://www.vectorlabs.com) containing 4,6-diamidino-2-phenylindole (Sigma-Aldrich) for nuclear labeling. Fluorescent images were examined and captured using a laser confocal microscope (Olympus, Tokyo, http://www.olympus-global.com).

Statistical Analysis

All statistical analyses were performed by unpaired Student's t test using GraphPad Prism software (GraphPad Software, La Jolla, CA, http://www.graphpad.com).

RESULTS

Robo4 Is Highly Expressed in Murine Hematopoietic Stem Cells and Immature Hematopoietic Progenitors

During a search for novel surface molecules expressed on HSCs, we noticed that cells in the hematopoietic and the nervous systems share a number of expressed genes [20–22]. These observations prompted us to investigate the expression of Robo family genes in the hematopoietic system. We first checked the expression of Robo family genes by RT-PCR. Interestingly, Robo4 was specifically expressed in murine KSL cells, which contain HSCs and immature hematopoietic progenitors. However, it was not expressed in lineage marker-positive (Lin^+) cells or various early hematopoietic progenitors, such as common myeloid progenitor, megakaryocyte/erythroid progenitor, granulocyte/monocyte progenitor, and common lymphoid progenitor (Fig. 1A, 1B). These data suggest that Robo4 is specifically expressed in murine HSCs and immature hematopoietic progenitors. In fact, $Robo4^+CD34^-KSL$ cells induced to differentiate in vitro no longer expressed Robo4 (supporting information Fig. 1), indicating that Robo4 is downregulated along with differentiation. Collectively, these results suggest that Robo4 is expressed in murine HSCs and immature hematopoietic progenitors, and its expression declines as the cells differentiate.

Analysis of Robo4 Expression by Flow Cytometry

We then generated a monoclonal antibody specific for Robo4 and examined its expression by flow cytometry (FACS). The antibody was specific to Robo4 (supporting information Fig. 2) and was not cross-reactive with other Robo family members (data not shown). Compatible with RT-PCR data, Robo4 was not expressed in lineage marker-positive cells in the murine BM (data not shown). As shown in Figure 2A, the highest expression of Robo4 was detected in the tip population of KSL cells (fraction a), which is enriched in HSCs. Furthermore, $CD34^-KSL$ cells, a highly enriched population of long-term HSCs, expressed higher Robo4 compared with $CD34^+KSL$ cells, an enriched fraction of short-term HSCs (Fig. 2B). Conversely, $Robo4^{high}KSL$ cells contained more $CD34^-KSL$ cells compared with $Robo4^{low/-}KSL$ cells (13.6% vs. 4.7%, respectively) (Fig. 2C). Taken together, these results confirm high expression of Robo4 in murine HSCs and immature hematopoietic progenitors.

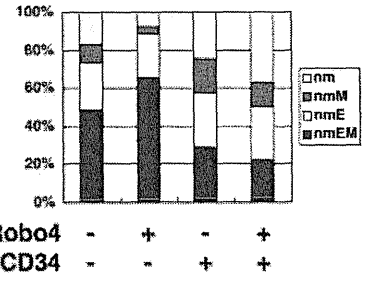

	nmEM	nmE	nmM	nm
$Robo4^-CD34^-$	48 ± 3	24 ± 3	10 ± 2	17 ± 3
$Robo4^+CD34^-$	66 ± 4 *	23 ± 2	4 ± 1	8 ± 2
$Robo4^-CD34^+$	29 ± 3 *	28 ± 4	18 ± 2	25 ± 3
$Robo4^+CD34^+$	23 ± 4	28 ± 4	13 ± 3	37 ± 5

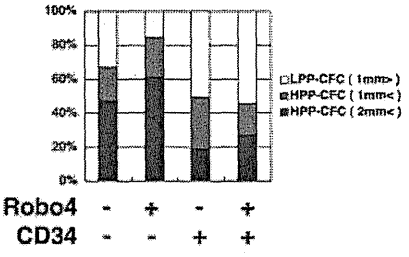

	HPP-CFC (> 2 mm)	HPP-CFC (1-2 mm)	LPP-CFC (< 1 mm)
$Robo4^-CD34^-$	47 ± 4	20 ± 2	33 ± 4
$Robo4^+CD34^-$	64 ± 5 *	21 ± 3	15 ± 2
$Robo4^-CD34^+$	19 ± 3 *	31 ± 3	51 ± 4
$Robo4^+CD34^+$	27 ± 5	19 ± 3	56 ± 3

Figure 3. Clonogenic activities of $Robo4^{high}$ hematopoietic stem/progenitor cells. **(A, B):** Murine c-$Kit^+Sca\text{-}1^+Lineage^-$ cells were clonally sorted into a 96-well dish (single cell per well) according to the expression of CD34 and Robo4 by fluorescence-activated cell sorting and subjected to clonogenic analyses. Two hundred cells were assessed for each sorted fraction, and the data are from three independent experiments. Colonies were assessed for their differentiation capacity **(A)** or colony size **(B)**. Graphs show percentage of colonies in each sorted fraction (total colony number was regarded as 100%). Tables show actual percentage of colonies (mean ± SD; $n = 3$). *, $p < .01$. $Robo4^+$ and $Robo4^-$ stand for $Robo4^{high}$ and $Robo4^{low/-}$ cells, respectively. LPP-CFCs were less than 1 mm in diameter; HPP-CFCs were more than 1 mm in diameter. Abbreviations: CFC, colony-forming cell; E, erythroid; HPP, high proliferating potential; LPP, low proliferating potential; m, macrophage; M, megakaryocyte; n, neutrophil; Robo, roundabout.

Expression of Robo4 Correlates with High Multipotentiality and Long-Term Repopulating Potential

We next examined the physiological relevance of Robo4 expression and the HSC activities. As shown in Figure 3A and 3B, $Robo4^{high}CD34^-KSL$ cells presented higher multilineage differentiation (shown as nmEM in Fig. 3A) and proliferative potential (shown as high proliferating potential-colony-forming cells in Fig. 3B) compared with other fractions. Interestingly, transplantation assays revealed that long-term repopulating activity of KSL cells was detected only in the $Robo4^{high}$ fraction and not in the $Robo4^{low/-}$ fraction (Fig. 4). These results suggest that higher expression of Robo4 defines a population of cells with higher capacities for mul-

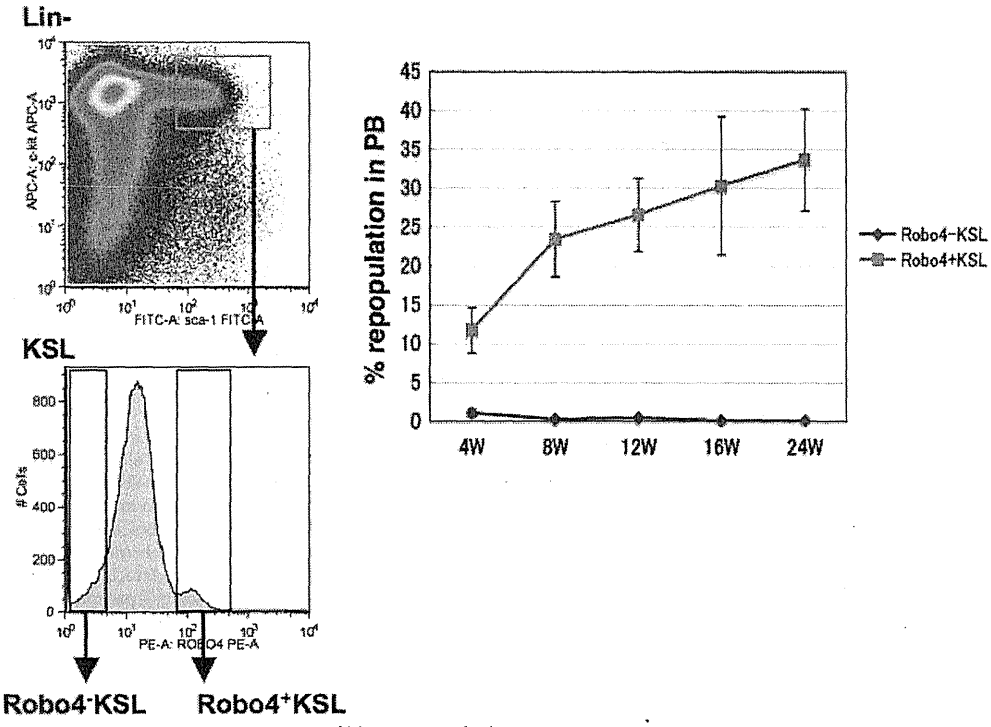

Figure 4. Long-term repopulating potential of Robo4^{high} and Robo4$^{low/-}$ hematopoietic stem/progenitor cells. KSL cells were sorted according to the expression of Robo4 and subjected to long-term repopulating assays as described in Materials and Methods. One hundred cells of each fraction were sorted and transplanted into each recipient mouse. The contribution of donor cells (percentage) in the recipients' PB was examined at the indicated time points. Data are mean ± SEM (n = 12 for each group). Representative data from three independent experiments are shown. Abbreviations: FITC, fluorescein isothiocyanate; KSL, c-Kit$^+$Sca-1$^+$Lineage$^-$; PB, peripheral blood; Robo, roundabout; W, weeks.

tilineage differentiation, proliferation, and long-term repopulation.

Slit2 Is Expressed in BM Stromal Cells and Induced in Osteoblasts by Myelosuppressive Stress

To obtain clues for the role of Robo4 in HSC regulation, we examined the expression of Slit2, a ligand for Robo4, by RT-PCR. As shown in Figure 5A, Slit family genes were not expressed in hematopoietic cells, such as KSL or Lin$^+$ cells. Interestingly, however, Slit2 was expressed in murine BM stromal cell lines (Fig. 5B) and the primary BM stromal cells (Fig. 5C). Of note, primary BM stromal cells also showed slight or moderate expression of Slit 1, Slit3, and Robo1. These results suggest that Slit2 is expressed in the BM microenvironment.

We went on to investigate the role of Slit2-Robo4 signaling in HSC physiology by examining the expression of Slit2 in the BM under a stress condition. We treated mice with a cytotoxic agent, 5-FU, and periodically monitored the expression of Slit2 in the BM by RT-PCR. Interestingly, Slit2 was transiently induced in the bone marrow on days 3–6 after 5-FU treatment, whereas Slit1 and Slit3 were not induced at all (Fig. 6A). Fractionation of BM cells by CD45 expression revealed that the induction occurred in CD45$^-$ cells, suggesting that Slit2 was induced in nonhematopoietic cells (Fig. 6B). Of note, a slight induction of Slit2 was also seen in CD45$^+$ cells after 9 days of 5-FU administration. The expression of Robo4 was also upregulated in the BM after 5-FU treatment, probably because of the concentration of immature hematopoietic cells in the BM (supporting information Fig. 3).

Given that Slit2 is induced in CD45$^-$ cells, we speculated that Slit2 might be induced in the BM niche in response to myelosuppressive stress. To test this hypothesis, we performed

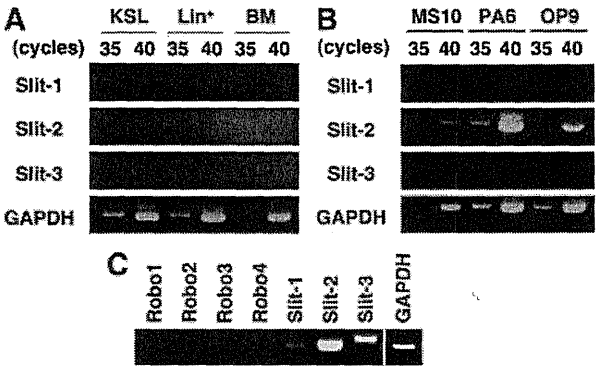

Figure 5. Expression of Slit genes in hematopoietic or BM stromal cells. **(A, B):** The expressions of Slit1–Slit3 genes were examined in KSL, Lin-positive, and whole BM cells **(A)** and various BM stromal cell lines **(B)** by reverse transcription-polymerase chain reaction (PCR). The amount of mRNA was normalized according to the expression of GAPDH. **(C):** The expression of Robo and Slit genes in primary BM stroma. Primary BM stromal cells were isolated by adherence to the culture dish, expanded, and subjected to PCR analysis. PCR was run for 40 cycles for Robo or Slit family genes and for 30 cycles for GAPDH. Abbreviations: BM, bone marrow; GAPDH, glyceraldehyde-3-phosphate dehydrogenase; KSL, c-Kit$^+$Sca-1$^+$Lineage$^-$; Lin, lineage marker; Robo, roundabout.

immunostaining of Slit2 in the BM treated with 5-FU for 3 days. As shown in Figure 6C, Slit2 was specifically induced in the osteoblasts at the endosteal surface of the bone marrow, where the HSC niche was reported to be located. Of note, expression of Slit2 was not detected in other places in the BM, such as endothelial cells (data not shown). These results suggest that

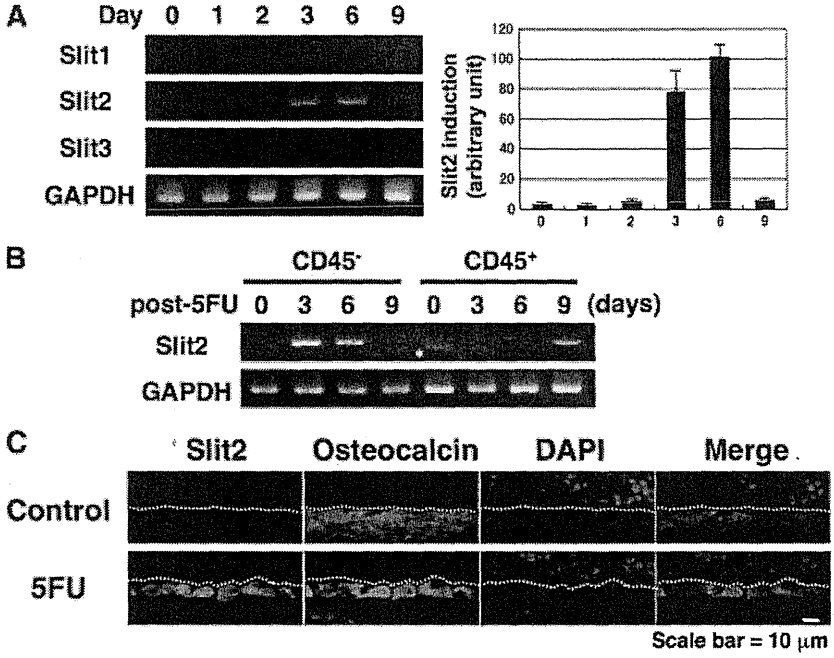

Figure 6. Induction of Slit2 in osteoblasts in response to myelosuppression. **(A):** Mice were treated with 5FU (150 mg/kg, i.p.), and the bone marrow (BM) cells were harvested at the indicated time points. Left panel: the expressions of Slit genes in whole BM cells were analyzed by reverse transcription (RT)-polymerase chain reaction (PCR). PCR was run for 35 cycles. Right panel: quantitative-RT-PCR for the Slit2 gene (mean ± SD; n = 3). **(B):** BM cells were harvested from 5FU-treated mice at the indicated time points. $CD45^+$ and $CD45^-$ cells were sorted by fluorescence-activated cell sorting and subjected to RT-PCR. PCR was run for 35 cycles. Asterisk indicates a nonspecific band. **(C):** Sections of femurs prepared from mice treated with 5FU for 3 days were immunostained with anti-Slit2 and osteocalcin antibodies. Nuclei were counterstained with DAPI. Broken lines indicate the margin of the bone surface. Abbreviations: DAPI, 4,6-diamidino-2-phenylindole; 5FU, 5-fluorouracil; GAPDH, glyceraldehyde-3-phosphate dehydrogenase.

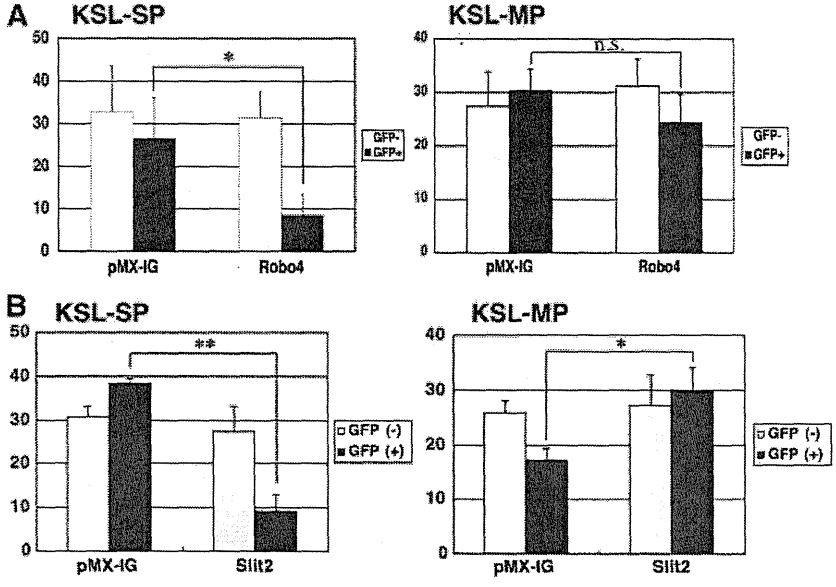

Figure 7. The role of Robo4/Slit2 signaling in SP-non-SP transition of HSCs. **(A, B):** Bone marrow (BM) mononuclear cells from mice treated with 5-fluorouracil (150 mg/kg, i.p.) were transduced with Robo4 **(A)**, Slit2 **(B)**, and mock vector (pMX-IG) by retrovirus. Equal numbers (1×10^4 cells) of infected and noninfected cells were sorted by fluorescence-activated cell sorting (FACS), mixed, and transplanted into lethally irradiated recipient mice. The BM cells were harvested after 3 months of transplantation, and the percentage of KSL-SP or KSL-MP in GFP^+ or GFP^- cells was analyzed by FACS (mean ± SD; n = 3). *, $p < .05$; **, $p < .01$. Abbreviations: GFP, green fluorescent protein; KSL, c-$Kit^+$$Sca\text{-}1^+$$Lineage^-$; MP, main population; n.s.; not significant by unpaired t test; Robo, roundabout; SP, side population.

Slit2-Robo4 signaling may play a role in HSC physiology in the osteoblastic niche upon myelosuppressive stress.

The Effect of Enhanced Robo4/Slit2 Signaling in SP to Non-SP Transition of HSCs

To gain more insight into the physiological role of Slit2/Robo4 signaling in HSCs, we enhanced Slit2/Robo4 signals by overexpressing Robo4 or Slit2 in the hematopoietic stem/progenitor cells and examined its effect on their SP phenotype. We retrovirally transduced Robo4 or Slit2 into the BM cells taken from 5-FU-treated mice and transplanted them into lethally irradiated recipients (Fig. 7A, 7B; supporting information Fig. 4). Robo4- or Slit2-expressing cells homed to and engrafted to the recipient's BM, albeit to a lesser extent compared with the mock control, and their contribution to the peripheral blood progressively decreased over time (supporting information Fig. 5). To our surprise, the percentage of KSL-SP was significantly lower in cells expressing Robo4 or Slit2 (green fluorescent protein $[GFP]^+$) compared with cells expressing mock vector (GFP^+) or nontransfected donor-derived cells (GFP^-) after 12 weeks of transplantation. In contrast, the percentage of KSL-MP was increased or remained constant in Slit2- or Robo4-transfected populations. On the basis of these observations, we speculated that Slit2/Robo4 signals might be acting to drive cells in KSL-SP into the KSL-MP or KSL-non-SP fraction. It is also possible that KSL-SP cells underwent apoptosis by enhanced Slit2/Robo4 signals. However, we speculate this is not the case, since we did not see any increased apoptosis in Robo4- or Slit2-overexpressing cells. In support of above hypothesis, Robo4 was highly expressed in KSL-SP cells (supporting information Fig. 6), indicating that these cells are sensitive to Slit2 stimuli. Taken together, these findings suggest that Slit2/Robo4 signaling promotes SP to non-SP transition of HSCs.

DISCUSSION

During the search for novel surface molecules expressed on primitive hematopoietic cells, we noticed that cells in the hematopoietic and nervous systems share a number of expressed genes. For example, we have previously reported that mKirre, which is abundantly expressed in brain and BM stromal cells, plays a critical role in maintaining HSC functions [20, 21]. Ephrins and their receptors, Ephs, are expressed in both the nervous and the hematopoietic systems, and they play critical roles in various aspects of neurogenesis and hematopoiesis [23–25]. Goolsby et al. also reported that hematopoietic progenitors express a set of neural genes [22]. These observations prompted us to focus on Robo family proteins, cell surface receptors that play a critical role in the nervous system. Within this family, Robo4 drew our particular attention, as the expression of Robo4 was specific to endothelial cells (ECs), and many HSC markers, such as CD34 and Flk1, were shared with ECs [26–28]. As expected, this study demonstrated that Robo4 is highly expressed in murine HSCs and immature hematopoietic progenitors. Moreover, transplantation experiments revealed that KSL cells with high Robo4 expression possessed higher long-term repopulating activity. These results demonstrate that the expression of Robo4 correlates with higher HSC capacities, such as long-term repopulation and differentiation to multiple lineages. During the course of our study, Forsberg et al. reported an extensive transcriptome analysis of LT-HSCs, ST-HSCs, and MPPs and showed that Robo4 is one of the differentially expressed genes among these three primitive hematopoietic cell populations [8]. In the current study, however, we demonstrated that the expression of Robo4 is highest in LT-HSCs not only among primitive hematopoietic cells, but also among all hematopoietic cells, including various progenitors and lineage marker-positive cells. In addition, we confirmed this observation on both the mRNA and the protein levels. Furthermore, we demonstrated that Robo4 could be used for isolating HSCs with long-term repopulating potential when combined with KSL phenotype.

Robo/Slit signaling acts as a repulsive axon guidance cue and inhibits migration of neuronal cells. In addition, Slit2 inhibits migration of endothelial cells through Robo4 [7]. On the basis of these published observations, it is reasonably speculated that Robo4 signaling inhibits HSC migration. It was also reported that *Drosophila* Slit/Robo signaling inhibits N-cadherin function in mammalian cells [29]. Since N-cadherin has been shown to play critical roles in the adhesion of HSCs and osteoblasts in the BM niche [9, 13], we also speculated that Robo4/Slit2 signaling might regulate HSC-osteoblast interaction upon myelosuppression. However, our preliminary analysis indicated that Slit2 did not inhibit migration of KSL cells toward SDF-1, and Robo4/Slit2 signaling did not inhibit N-cadherin-mediated adhesion in mammalian cells (unpublished observation). These data do not necessarily exclude the possibility that Robo4/Slit2 system is involved in migration or adhesion of HSCs in the physiological settings, and additional studies using gene-deficient animals will be required to unravel the precise roles of Robo4/Slit2 signaling in the HSC dynamics.

In a similar vein as the regulation of HSCs by the BM niche, it is intriguing that enhanced Slit2/Robo4 signaling resulted in the decreased residence of HSCs in the SP fraction. The SP phenotype is defined as a cell population with a high capacity of Hoechst 33342 dye efflux, and the efflux of Hoechst dye is accomplished by one of the ATP-binding cassette transporters, ABCG2/Bcrp-1 [30]. A gene disruption study in mice revealed that Bcrp-1 is absolutely required for the SP phenotype [31]; however, the expression of Bcrp-1 is equally observed in SP and non-SPs of $CD34^{-}$KSL cells, suggesting that the function of Bcrp-1 is regulated by other factors [32]. Our finding that enhanced Slit2/Robo4 signaling led to decreased HSC residence in the SP fraction indicates that Slit2 could be a candidate factor regulating the Bcrp-1 function. In this regard, the induction of Slit2 in osteoblasts upon myelosuppression is of particular interest. It has been reported that HSCs are recruited from the SP to the non-SP fraction on days 4–6 after 5-FU treatment [13]. The induction of Slit2 occurs on days 3–6 after 5-FU administration, which precedes or coincides with the SP to non-SP transition of HSCs. These data suggest that Slit2 induced in the BM niche upon myelosuppression acts on HSCs through Robo4 and may play a critical role in their transition from the SP to the non-SP fraction. Preliminary analysis of Robo4-deficient mice showed that there is only a slight difference, if any, in the proportion of KSL-SP cells between knockout and wild-type animals (data not shown). This suggests that other redundant pathways, in addition to Robo4, could regulate the SP to non-SP transition of HSCs, and further detailed analysis of Robo4-deficient mice would be required to unravel precise roles of Robo4 in vivo. Considering a well-recognized role of Robo/Slit signaling in cellular migration [1], it is also tempting to speculate that Slit2 might be acting to induce HSC migration out of the niche in response to myelosuppression.

SUMMARY

We identified Robo4 as a receptor expressed on hematopoietic stem cells that is potentially involved in the regulation of the SP phenotype. Revealing the physiological role of Robo4/Slit2 signaling would lead to a better understanding of HSC homeostasis in the BM niche.

ACKNOWLEDGMENTS

We thank N. Watanabe, T. Shibata, and S. Saito (FACS Core Laboratory, Institute of Medical Science, University of Tokyo) for FACS sorting, and Dr. Dovie R. Wylie for language assistance. This work was supported in part by a grant from the Ministry of Education, Culture, Sports, Science and Technology of Japan. H.N. is currently affiliated with the Division of Hematology, Department of Internal Medicine, Keio University School of Medicine, Tokyo, Japan.

DISCLOSURE OF POTENTIAL CONFLICTS OF INTEREST

J.P.H. was employed by R&D Systems.

REFERENCES

1 Wong K, Park HT, Wu JY et al. Slit proteins: Molecular guidance cues for cells ranging from neurons to leukocytes. Curr Opin Genet Dev 2002;12:583–591.

2 Rajagopalan S, Nicolas E, Vivancos V et al. Crossing the midline: Roles and regulation of Robo receptors. Neuron 2000;28:767–777.

3 Brose K, Bland KS, Wang KH et al. Slit proteins bind Robo receptors and have an evolutionarily conserved role in repulsive axon guidance. Cell 1999;96:795–806.

4 Wu JY, Feng L, Park HT et al. The neuronal repellent Slit inhibits leukocyte chemotaxis induced by chemotactic factors. Nature 2001;410:948–952.

5 Wang B, Xiao Y, Ding BB et al. Induction of tumor angiogenesis by Slit-Robo signaling and inhibition of cancer growth by blocking Robo activity. Cancer Cell 2003;4:19–29.

6 Huminiecki L, Gorn M, Suchting S et al. Magic roundabout is a new member of the roundabout receptor family that is endothelial specific and expressed at sites of active angiogenesis. Genomics 2002;79:547–552.
7 Park KW, Morrison CM, Sorensen LK et al. Robo4 is a vascular-specific receptor that inhibits endothelial migration. Dev Biol 2003;261:251–267.
8 Forsberg EC, Prohaska SS, Katzman S et al. Differential expression of novel potential regulators in hematopoietic stem cells. PLoS Genet 2005;1:e28.
9 Zhang J, Niu C, Ye L et al. Identification of the haematopoietic stem cell niche and control of the niche size. Nature 2003;425:836–841.
10 Calvi LM, Adams GB, Weibrecht KW et al. Osteoblastic cells regulate the haematopoietic stem cell niche. Nature 2003;425:841–846.
11 Goodell MA, Brose K, Paradis G et al. Isolation and functional properties of murine hematopoietic stem cells that are replicating in vivo. J Exp Med 1996;183:1797–1806.
12 Goodell MA, Rosenzweig M, Kim H et al. Dye efflux studies suggest that hematopoietic stem cells expressing low or undetectable levels of CD34 antigen exist in multiple species. Nat Med 1997;3:1337–1345.
13 Arai F, Hirao A, Ohmura M et al. Tie2/angiopoietin-1 signaling regulates hematopoietic stem cell quiescence in the bone marrow niche. Cell 2004;118:149–161.
14 Tulin EE, Onoda N, Maeda M et al. A novel secreted form of immune suppressor factor with high homology to vacuolar ATPases identified by a forward genetic approach of functional screening based on cell proliferation. J Biol Chem 2001;276:27519–27526.
15 Nakano T, Kodama H, Honjo T. Generation of lymphohematopoietic cells from embryonic stem cells in culture. Science 1994;265:1098–1101.
16 Nakajima H, Shibata F, Fukuchi Y et al. Immune suppressor factor confers stromal cell line with enhanced supporting activity for hematopoietic stem cells. Biochem Biophys Res Commun 2006;340:35–42.
17 Ema H, Morita Y, Yamazaki S et al. Adult mouse hematopoietic stem cells: Purification and single-cell assays. Nat Protoc 2006;1:2979–2987.
18 Kitamura T, Koshino Y, Shibata F et al. Retrovirus-mediated gene transfer and expression cloning: Powerful tools in functional genomics. Exp Hematol 2003;31:1007–1014.
19 Morita S, Kojima T, Kitamura T. Plat-E: An efficient and stable system for transient packaging of retroviruses. Gene Ther 2000;7:1063–1066.
20 Ueno H, Sakita-Ishikawa M, Morikawa Y et al. A stromal cell-derived membrane protein that supports hematopoietic stem cells. Nat Immunol 2003;4:457–463.
21 Tamura S, Morikawa Y, Hisaoka T et al. Expression of mKirre, a mammalian homolog of *Drosophila* kirre, in the developing and adult mouse brain. Neuroscience 2005;133:615–624.
22 Goolsby J, Marty MC, Heletz D et al. Hematopoietic progenitors express neural genes. Proc Natl Acad Sci U S A 2003;100:14926–14931.
23 Klein R. Eph/ephrin signaling in morphogenesis, neural development and plasticity. Curr Opin Cell Biol 2004;16:580–589.
24 Augustin HG, Reiss Y. EphB receptors and ephrinB ligands: Regulators of vascular assembly and homeostasis. Cell Tissue Res 2003; 314:25–31.
25 Suenobu S, Takakura N, Inada T et al. A role of EphB4 receptor and its ligand, ephrin-B2, in erythropoiesis. Biochem Biophys Res Commun 2002;293:1124–1131.
26 Silvestri F, Banavali S, Baccarani M et al. The CD34 hemopoietic progenitor cell associated antigen: Biology and clinical applications. Haematologica 1992;77:265–273.
27 Shalaby F, Rossant J, Yamaguchi TP et al. Failure of blood-island formation and vasculogenesis in Flk-1-deficient mice. Nature 1995;376: 62–66.
28 Ziegler BL, Valtieri M, Porada GA et al. KDR receptor: A key marker defining hematopoietic stem cells. Science 1999;285:1553–1558.
29 Rhee J, Mahfooz NS, Arregui C et al. Activation of the repulsive receptor Roundabout inhibits N-cadherin-mediated cell adhesion. Nat Cell Biol 2002;4:798–805.
30 Zhou S, Schuetz JD, Bunting KD et al. The ABC transporter Bcrp1/ABCG2 is expressed in a wide variety of stem cells and is a molecular determinant of the side-population phenotype. Nat Med 2001;7: 1028–1034.
31 Zhou S, Morris JJ, Barnes Y et al. Bcrp1 gene expression is required for normal numbers of side population stem cells in mice, and confers relative protection to mitoxantrone in hematopoietic cells in vivo. Proc Natl Acad Sci U S A 2002;99:12339–12344.
32 Morita Y, Ema H, Yamazaki S et al. Non-side-population hematopoietic stem cells in mouse bone marrow. Blood 2006;108:2850–2856.

See www.StemCells.com for supporting information available online.

GASTROENTEROLOGY 2010;138:1312–1320

Effects of Ghrelin Administration After Total Gastrectomy: A Prospective, Randomized, Placebo-Controlled Phase II Study

SHINICHI ADACHI,* SHUJI TAKIGUCHI,* KAZUYUKI OKADA,‡ KAZUYOSHI YAMAMOTO,* MAKOTO YAMASAKI,* HIROSHI MIYATA,* KIYOKAZU NAKAJIMA,* YOSHIYUKI FUJIWARA,* HIROSHI HOSODA,§ KENJI KANGAWA,§ MASAKI MORI,* and YUICHIRO DOKI*

*Department of Gastroenterological Surgery, Osaka University Graduate School of Medicine, Osaka; ‡Department of Surgery, Suita Municipal Hospital, Osaka; and §Department of Biochemistry, National Cardiovascular Center Research Institute, Osaka, Japan

BACKGROUND & AIMS: Body weight (BW) loss and reduction of blood ghrelin level are commonly observed after total gastrectomy (TG). A prospective study was designed to elucidate whether exogenous ghrelin administration prevents postoperative BW loss by improving appetite and oral food intake in patients with gastric cancer after undergoing TG. **METHODS:** In this randomized phase II study, 21 patients undergoing TG were assigned to a ghrelin (11 patients) or placebo group (10 patients). They received intravenous infusion of synthetic human ghrelin (3 μg/kg) or saline twice daily for 10 days after starting oral food intake following surgery. Changes in BW, appetite visual analog scale score, food intake calories, body composition, basal metabolic rate, and various blood test results were evaluated. **RESULTS:** Excluding one patient who developed profound diaphoresis during ghrelin infusion, 20 patients completed the study. Food intake and appetite were significantly higher with ghrelin compared with placebo (average, 13.8 vs 10.4 kcal/kg/day [$P = .030$] and 5.7 vs 3.9 cm [$P = .032$], respectively). BW loss was significantly lower in the ghrelin than in the placebo group (−1.4% vs −3.7%; $P = .044$). Fat mass, lean body mass, and basal metabolic rate decreased significantly in the placebo group; however, the reductions in lean body mass and basal metabolic rate were not significant in the ghrelin group, although that of fat mass was significant. **CONCLUSIONS: Short-term administration of synthetic ghrelin was safe and successfully lessened postoperative BW loss and improved appetite and food intake after TG.**

Keywords: Ghrelin; Total Gastrectomy; Gastric Cancer; Body Weight Loss.

Body weight loss is common and a serious outcome in patients with gastric cancer who have undergone total gastrectomy. It correlates well with decline in postoperative quality of life and is the most reliable indicator of malnutrition, which impairs immune function, infection susceptibility, and survival.[1–3] Although various mechanisms have been considered, such as perturbation of absorption due to reduced pancreatic excretion,[4,5] decrease of gastric acid level,[6] reflux esophagitis,[7] intestinal floral alteration,[8] and increased peristalsis and diarrhea,[9] reduced food intake[10,11] is the most conceivable explanation for body weight loss after total gastrectomy. Therefore, surgeons dealing with gastric cancers have tried to increase food intake by producing a gastric substitute, such as a jejunal pouch, but such procedures have not always been successful.[12] Another study indicated that the majority of patients with total gastrectomy could eat food as much as healthy subjects under a regulated program.[13] Our own experience indicates that some patients do not show significant body weight loss after total gastrectomy by resorting to small but frequent meals. These changes suggest that reduced food intake after total gastrectomy could not be simply explained by loss of storage volume due to gastrectomy, but rather reflect a disturbance of eating activity through an unknown mechanism.

The 28-amino acid peptide ghrelin is the endogenous ligand for the growth hormone (GH) secretagogue receptor 1a, which stimulates GH release from the pituitary gland.[14] The majority of ghrelin is produced by X/A-like cells of the oxyntic glands in the stomach, and a smaller amount is secreted from other organs, such as the intestine, pancreas, kidney, and hypothalamus.[15,16] Ghrelin has various physiologic functions in addition to secretion of GH, such as promoting the appetite signal in the hypothalamus (in contrast to leptin),[17] stimulating gastrointestinal activity (such as peristalsis, gastric acid secretion, and pancreatic excretion through the vagal nerves),[18] and regulation of fat metabolism.[19] In addition, ghrelin mitigates proinflammatory cytokine production and attenuates the stress signal.[20] Among the pleiotropic functions of ghrelin, this peptide is the only gastrointestinal hormone known to stimulate appetite. A randomized double-blind study of healthy volunteers

Abbreviations used in this paper: ANOVA, analysis of variance; BMR, body metabolic rate; GH, growth hormone; IGF, insulin-like growth factor.

0016-5085/10/$36.00
doi:10.1053/j.gastro.2009.12.058

showed that ghrelin enhances appetite and increases food intake.[21,22] Thereafter, several clinical trials of patients with heart failure,[23] pulmonary disease,[24] and cancer cachexia[25] concluded that ghrelin successfully improved the diseases along with increased oral food intake and body weight. In the field of surgical treatment for obesity, reduction in ghrelin levels after sleeve gastrectomy is associated with successful body weight loss and appetite suppression.[26] Taken together, the discovery of ghrelin allows the proposal of a new concept, body weight regulation by the stomach, which could be applied to various diseases with malnutrition.

We reported previously that serum ghrelin levels decreased to 10% to 20% of the preoperative level immediately after total gastrectomy[27,28] and did not recover thereafter, accompanied by approximately 20% body weight loss.[10,12,27] These findings suggest that loss of ghrelin could be involved in body weight loss observed after total gastrectomy. The present prospective, randomized, placebo-controlled phase II study investigated the effects of exogenous ghrelin administration on postoperative body weight loss by improving appetite and oral food intake in patients with gastric cancer who had undergone total gastrectomy. We report here the successful results of the study, and further use of ghrelin for these patients is discussed.

Patients and Methods

Patients

Twenty-one patients who underwent total gastrectomy at Osaka University Hospital between June 2006 and June 2008 were enrolled in the study. The inclusion criteria were as follows: (1) adenocarcinoma of the stomach confirmed by histopathologic examination, (2) preoperative clinical staging with less than stage II (International Union Against Cancer TNM stage classification), (3) curative surgical treatment (R0) (ie, total gastrectomy with D1 or D2 lymph node dissection), and (4) age between 20 and 80 years. The exclusion criteria were the presence of any of the following: (1) cardiopulmonary, liver, or renal dysfunction; (2) active dual malignancy; (3) pregnancy; (4) past history of gastrointestinal surgery; and (5) postoperative complications after total gastrectomy that could affect oral food intake, such as anastomotic leakage, pancreatitis, and mechanical ileus. Twenty-one patients were randomized by sealed envelope and divided into 2 study groups. The center office generated the allocation sequence and enrolled and assigned the patients to the 2 groups, and the random allocation sequence was concealed until interventions were assigned. Eleven patients received repeated administrations of ghrelin (ghrelin group), and 10 patients received repeated administrations of pure saline (placebo group). The study was approved by the Osaka University Ethics Committee, and all patients gave written informed consent before study entry in accordance with the Declaration of Helsinki. The study was registered at UMIN (http://www.umin.ac.jp; clinical trial no. UMIN000001925).

Preparation of Synthetic Human Ghrelin

Synthetic human ghrelin, which consists of 99.4% acyl ghrelin and 0.6% des-acyl ghrelin, based on analysis by high-performance liquid chromatography, was obtained from Peptide Institute Inc (Osaka, Japan). Endotoxin examinations and the pyrogen test for ghrelin solutions were conducted as described previously.[29] Synthetic human ghrelin was dissolved in distilled water with 3.75% D-mannitol and sterilized by passage through a filter. Ghrelin solution was stored in 2-mL volumes, each containing 210 μg. These solutions were stored at −20°C in sterile vials until preparation of ghrelin for administration.

End Points and Study Protocol

The primary end point of this study was an increase in orally ingested calories following ghrelin administration. The secondary end points included changes in body weight, appetite, body composition, basal metabolism, and blood tests. The study design is summarized in Figure 1*A*. The patient usually started oral food intake of rice porridge between postoperative day 5 and postoperative day 7. All patients were served standard postoperative meals, but they were always allowed to receive extra food when they desired. In the following 10 days after starting oral food intake, intravenous drip infusion of synthetic human ghrelin (3 μg/kg) or placebo was administered twice a day (before breakfast and before dinner). Ghrelin solution and placebo (pure saline) were added to a 50-mL saline bottle, which was intravenously infused over a 30-minute period. The same amount of ghrelin was administered through intravenous infusion during the 10-day treatment; the dose was calculated based on the body weight on the day before oral food intake. During the study period, the same protocol of intravenous infusion and the same menu of meals were provided for the 2 groups. The composition of the intravenous infusion fluid was 43.0 g glucose, 35 mEq Na, 20 mEq K, 35 mEq Cl, and 20 mEq lactate in 1000 mL. The protocol of intravenous infusion was 2000 mL/day from postoperative day 1 to postoperative day 7 and 1000 mL/day from postoperative day 8 to postoperative day 14. The study was performed in a single-blind manner; patients without knowledge of their treatment assessed the amount of food intake, appetite, and body weight every day during the treatment by themselves without any intervention by the hospital staff. Food intake calories based on the food weight measured by the patient, including standard meal and extra foods, were calculated by dietitians using a calorimeter. Preprandial appetite at every meal was scored by the visual analog scale (possible scales, 0–10 cm) recorded in the account sheet by each

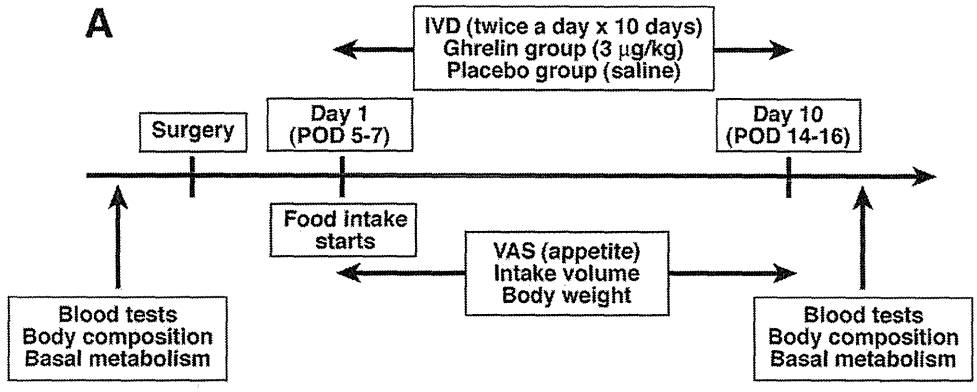

POD; postoperative day, VAS; visual analogue scale; IVD; intravenous drip

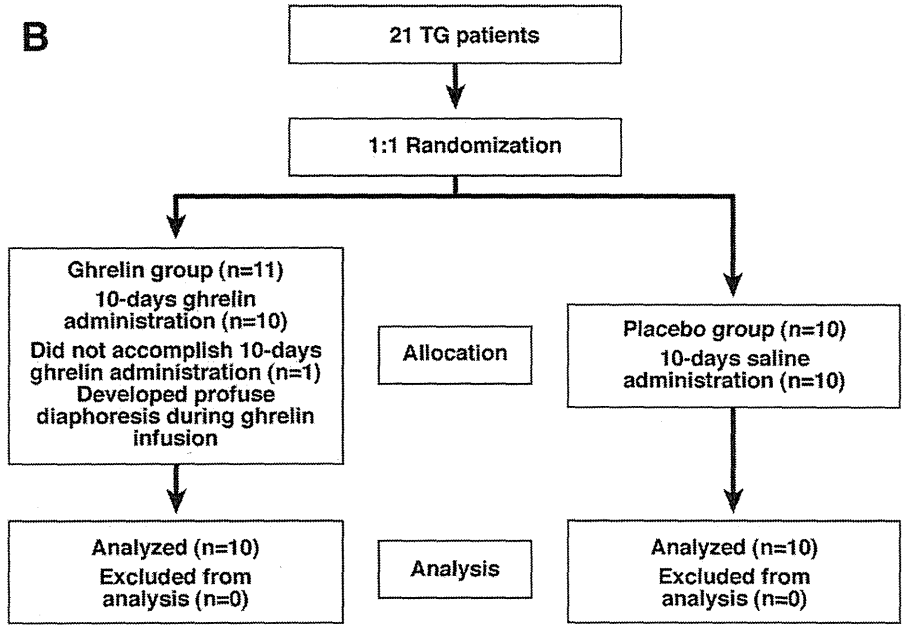

Figure 1. Study protocol and flow diagram.

patient. Body weight was measured with a beam scale to the nearest 0.1 kg, with patients standing barefoot and in light clothing.

Body composition was measured by using dual-energy x-ray absorptiometry (Hologic QDR-2000 instrument; Hologic Inc, Waltham, MA) to assess changes in lean body mass, fat mass, and bone mineral content before and after protocol treatment. The whole body was scanned in the single-beam mode, and the results were analyzed with body composition software. Basal metabolism was measured by using a metabolic analyzer (MedGem metabolic analyzer; HealtheTech, Golden, CO) to assess changes in basal metabolism before and after treatment. All subjects breathed through the MedGem using a disposable, scuba-type mouthpiece. During the measurement, oxygen consumption (VO_2) and body metabolic rate (BMR) were continuously and electronically recorded on a personal computer.

Blood Sampling and Assay

Blood samples were collected from patients before breakfast after an overnight fast, transferred into chilled tubes, stored on ice during collection, centrifuged, serum separated, and stored at −50°C until assay. Insulin-like growth factor (IGF)-I levels were measured by IGF-I IRMA "Daiichi" (TFB, Inc, Tokyo, Japan). Norepinephrine was measured using high-performance liquid chromatography (Tosoh Co, Tokyo, Japan). Cortisol and insulin were measured using the Cortisol Kit "TFB" (TFB, Inc, Tokyo, Japan) and chemiluminescent enzyme immunoassay (Fujirebio, Inc, Tokyo, Japan), respectively. Serum GH and leptin were

measured using GH Kit "Daiichi" (TFB, Inc, Tokyo, Japan) and Human Leptin RIA Kit (Linco Research Inc, St Charles, MO), respectively.

Sample Size Calculation and Statistical Analysis

We estimated that the difference in the effect of ghrelin or placebo on oral food intake calories should be at least 25% assuming 1200 and 1500 kcal/day in the placebo and ghrelin groups, respectively, with ±200 kcal for each SD. To analyze the difference in the effects in the ghrelin and placebo groups using Student *t* test, the study group should comprise at least 16 subjects, with a 5% α value and statistical power of 80%. Assuming that 20% of subjects in each group would not complete the study, the total number of subjects required in this study was estimated at 20.

Numerical values are expressed as mean ± SD unless otherwise indicated. Differences in parameters between the placebo and ghrelin groups were tested by Student *t* test or Mann-Whitney *U* test. Changes in parameters before and after total gastrectomy were tested statistically by the paired *t* test or Wilcoxon signed rank test. Changes in parameters between the 2 groups during the 10 days of follow-up were tested for significance by repeated-measures analysis of variance (ANOVA). A *P* value of <.05 was considered statistically significant. SAS for Windows software version 9 (SAS Institute, Inc, Cary, NC) was used to conduct repeated-measures ANOVA, whereas StatView version 5.0 (SAS Institute, Inc) was used for other tests.

Results

Patient Characteristics

The study flow diagram is summarized in Figure 1*B*. One of the 11 patients (9.1%) in the ghrelin group developed profuse diaphoresis during ghrelin infusion, equivalent to grade 1 by National Cancer Institute Common Terminology Criteria for Adverse Events version 3.0. Accordingly, we decided to stop ghrelin administration and the patient was excluded from further analysis. The 10-day course of ghrelin administration was well tolerated by the remaining 10 patients without any adverse events, although some reported transient periods of feeling warm and/or peristalsis during ghrelin infusion. Table 1 summarizes the clinical background of the 20 patients who completed the study. There was no significant difference in age, sex, body weight, body mass index, and clinical stage of gastric cancer between the 2 groups.

Table 1. Patient Characteristics

Parameter	Ghrelin group	Placebo group	*P* value
n	10	10	
Age (*y*)	64.8 ± 10.4	61.6 ± 8.4	.46
Sex (male/female)	7/3	4/6	.19
Body weight (*kg*)	62.2 ± 13.6	62.9 ± 11.5	.89
Body mass index (kg/m^2)	23.1 ± 3.1	24.5 ± 3.8	.36
Procedure (LATG/COTG)	8/2	9/1	.54
Clinical TMN stage			
T (T1/T2/T3/T4)	7/1/2/0	8/2/0/0	.49
N (N0/N1/N2)	9/1/0	9/1/0	1.00
Stage (I/II/III/IV)	8/2/0/0	10/0/0/0	.15

LATG, laparoscopic assisted total gastrectomy; COTG, conventional open total gastrectomy.

Effects of Ghrelin on Appetite, Food Intake, and Body Weight Loss

Appetite, oral food intake, and body weight were recorded by the patients throughout 10 days of ghrelin/saline administration. During this period, the patients in the 2 groups received the same amount (ie, volume and calories) of intravenous infusion. The mean appetite visual analog scale score was significantly higher in the ghrelin group than the placebo group during the 10-day period (Figure 2*A*; repeated-measures ANOVA, $P = .032$).

Food intake calories (kcal/kg/day) during the 10-day period were significantly higher in the ghrelin group than in the placebo group (Figure 2*B*; repeated-measures ANOVA, $P = .030$). Food intake gradually increased at an earlier period of food intake and was then unchanged thereafter; both groups showed a similar difference throughout the 10-day period. The mean intake calorie over the 10-day period was 13.8 and 10.4 kcal/kg/day for the ghrelin and placebo groups, and ghrelin administration accounted for about 32.7% of the increase.

Body weight loss was calculated in reference to the first day of oral food intake. During this period, body weight gradually decreased in both groups, although the loss was more evident in the placebo group. At the end of the intravenous drip protocol (Day 10), body weight loss was −3.7% for the placebo group but only −1.4% for the ghrelin group. For the 10-day period, body weight loss of the ghrelin group was less than that of the placebo group (Figure 2C; repeated-measures ANOVA, $P = .044$).

Effects of Ghrelin on Body Composition and Basal Metabolism

Consistent with the body weight changes, both lean body mass and fat mass decreased gradually during the study period. The mean change in fat mass was −8.8% (14,100 ± 5400 to 12,900 ± 5200 g) and −7.6% (19,000 ± 8400 to 17,700 ± 8300 g) for the ghrelin and placebo groups, respectively. The reduction was statistically significant for each group (Figure 3*A*; $P < .001$). The mean change in lean body mass in the placebo group was −7.8% (41,800 ± 6500 to 38,500 ± 5700 g), which was also significant (Figure 3*B*; $P < .001$); however, the change in the ghrelin group was only −2.9% (44,600 ± 10,500 to 43,200 ± 9600 g, Figure 3*B*; $P = .076$). Figure 3C shows the BMR values before and after total gastrectomy. BMR decreased significantly after total gastrectomy in the placebo group (21.8 ± 4.0 to 19.4 ± 3.4

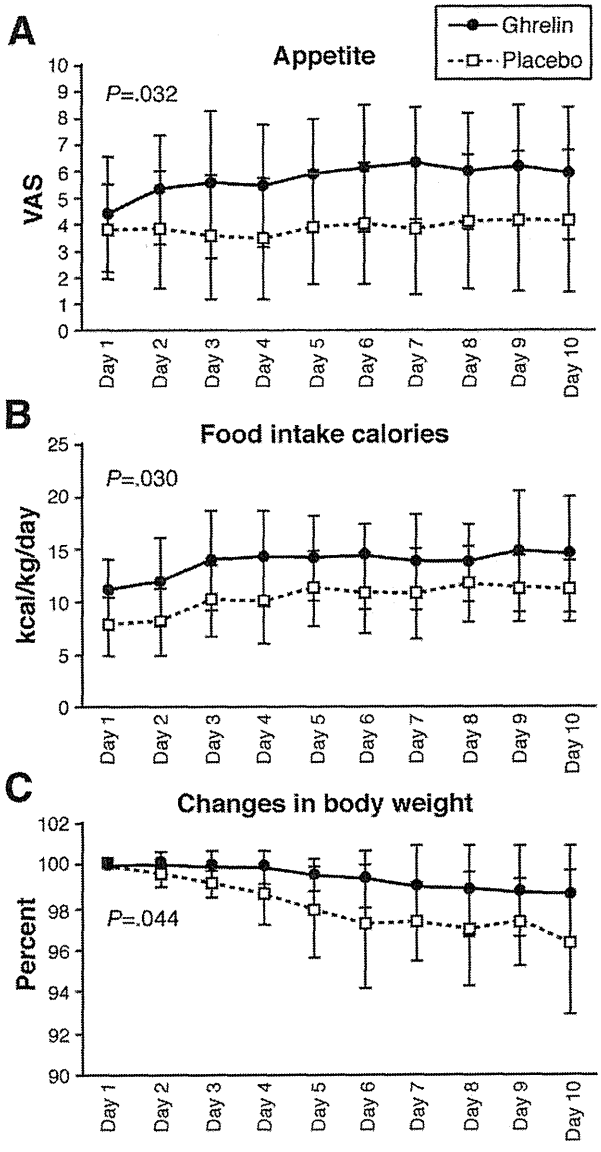

Figure 2. Serial changes in appetite, food intake, and body weight during the 10-day study in the ghrelin and placebo groups. Data are expressed as the mean ± SD of visual analog scale scores of (*A*) preprandial appetite at every meal, (*B*) daily total food intake calories per body weight (kcal/kg/day), and (*C*) percent body weight relative to the first day of oral intake in the ghrelin and placebo groups. The visual analog scale score throughout the study period, which was evaluated by repeated-measures ANOVA, was significantly higher in the ghrelin group than in the placebo group (5.7 vs 3.9 cm; $P = .032$). Likewise, food intake calories were significantly higher in the ghrelin group than in the placebo group (average, 13.8 vs 10.4 kcal/kg/day; repeated-measures ANOVA, $P = .030$). Body weight loss in the ghrelin group was significantly lower than in the placebo group (−1.4% vs −3.7%; repeated-measures ANOVA, $P = .044$).

kcal/kg; $P = .023$). In contrast, the reduction in BMR in the ghrelin group was smaller, and the difference between before and after treatment was not significant (22.6 ± 6.1 to 21.4 ± 6.0 kcal/kg; $P = .20$).

Blood Tests and Hormone Assays

Finally, we compared the results of certain blood tests that reflect the nutritional status and hormones (hemoglobin, total protein, albumin, total cholesterol, triglyceride, leptin, GH, cortisol, norepinephrine, insulin, and IGF-I) both before and after the 10-day period (Table 2). In the early recovery phase, the parameters associated with nutrition did not change in the placebo group but significantly improved in the ghrelin group. Leptin levels decreased significantly in both groups after total gastrectomy, consistent with the reduction in fat mass. On the other hand, there was no significant change in GH, cortisol, norepinephrine, insulin, and IGF-I levels after treatment in both groups.

Discussion

Body weight loss is a common finding in patients who undergo gastrectomy for gastric cancer, which not

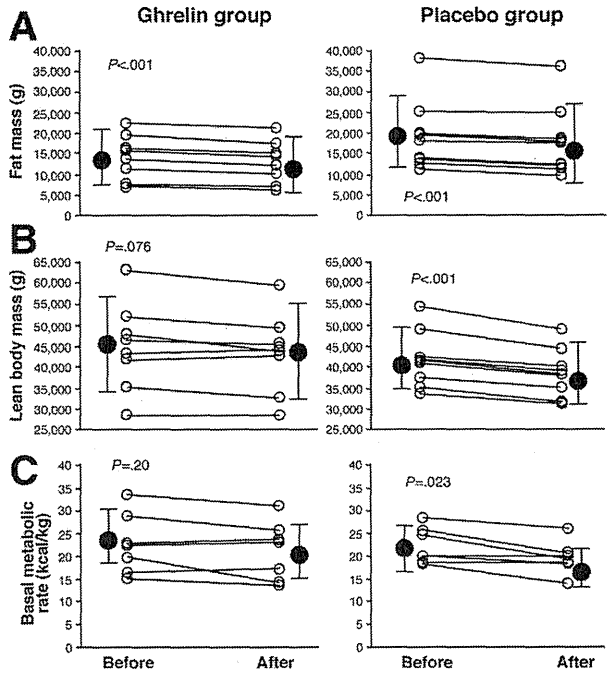

Figure 3. Body composition and basal metabolic rate before and after the study in the ghrelin and placebo groups. (*A*) Fat mass and (*B*) lean body mass measured by dual-energy x-ray absorptiometry and (*C*) basal metabolic rate were determined before and after the 10-day study. Changes for each patient (*open circles*) and the whole group (*closed circles*, ±SD) are shown for the ghrelin and placebo groups. The reductions in all 3 parameters were statistically significant in the placebo group by Student *t* test (fat mass, 19,000 ± 8400 to 17,700 ± 8300 g [$P < .001$]; lean body mass, 41,800 ± 6500 to 38,500 ± 5700 g [$P < .001$]; BMR, 21.4 ± 6.0 to 19.4 ± 3.4 kcal/kg [$P = .023$]). In the ghrelin group, the reduction of fat mass was significant while that of lean body mass and BMR was less than in the placebo group and not statistically significant (fat mass, 14,100 ± 5400 to 12,900 ± 5200 g [$P < .001$]; lean body mass, 44,600 ± 10,500 to 43,200 ± 9600 g [$P = .076$]; BMR, 22.6 ± 6.1 to 21.4 ± 6.0 kcal/kg [$P = .20$]).

Table 2. Results of Laboratory Tests

	Ghrelin group	Placebo group
Hemoglobin (*g/dL*)		
Before	12.2 ± 0.8	12.7 ± 2.4
After	11.8 ± 1.1	11.7 ± 1.4
Total protein (*g/dL*)		
Before	5.7 ± 0.3	6.0 ± 0.7
After	6.6 ± 0.4[a]	6.4 ± 0.3
Albumin (*g/dL*)		
Before	3.1 ± 0.2	3.4 ± 0.6
After	3.5 ± 0.4[a]	3.5 ± 0.2
Total cholesterol (*mg/dL*)		
Before	148 ± 43	176 ± 26
After	174 ± 37[a]	164 ± 32
Triglyceride (*mg/dL*)		
Before	82 ± 47	77 ± 29
After	113 ± 32[a]	99 ± 44
Leptin (*ng/mL*)		
Before	3.1 ± 1.4	7.9 ± 6.7
After	1.2 ± 0.4[b]	4.1 ± 4.0[b]
GH (*ng/mL*)		
Before	0.87 ± 1.5	0.62 ± 0.8
After	0.55 ± 0.7	1.65 ± 2.7
Cortisol (*μg/dL*)		
Before	18.6 ± 4.8	16.9 ± 4.6
After	17.0 ± 4.0	17.9 ± 6.7
Norepinephrine (*pg/mL*)		
Before	314 ± 132	294 ± 171
After	366 ± 122	269 ± 158
Insulin (*μIU/mL*)		
Before	6.1 ± 3.5	10.3 ± 5.5
After	5.1 ± 2.5	6.5 ± 6.0
IGF-I (*ng/mL*)		
Before	108 ± 33	92 ± 36
After	85 ± 53	76 ± 37

[a]$P < .05$, [b]$P < .01$ (paired *t* test; before vs after).

only associates with various pathologic conditions but also affects patients' social activity. Therefore, postoperative body weight loss needs to be investigated thoroughly, especially in Japan, where early gastric cancer accounts for more than 50% of the total incidence of gastric cancer,[30] and the 5-year survival rate of early gastric cancer is more than 90%.[31] Previous studies reported that body weight loss after total gastrectomy was approximately 15% to 20% of the preoperative weight.[10,12,27] Because the incidence of gastric cancer is associated with low body weight in not only Japan and Asian countries but also in the Western world, the estimated average body mass index after total gastrectomy is expected to be 18 to 20 kg/m^2, which is lower than the ideal body mass index. The correlation between low body weight and long-term survival rate has not been analyzed thoroughly even in healthy individuals. A large cohort study of healthy Japanese subjects surveyed over 10 years concluded that a body mass index less than 19 kg/m^2 was associated with high mortality risk at an odds ratio of 2.26 due to various diseases, including infectious, cardiovascular, and malignant diseases.[3] Although there are no concrete data for patients who undergo gastrectomy, these patients could be at risk for a higher mortality rate due to low body weight. Based on this background, the major purpose of this study was to minimize postoperative body weight loss by ghrelin administration through up-regulation of GH secretion and appetite.

At the end of the 10-day study period, ghrelin reduced more than half of postoperative body weight loss from −3.7% in the placebo group to −1.4% in the ghrelin group. Although this is a limited result in the early postoperative period, which is associated with the most profound body weight loss, to the best of our knowledge, ghrelin administration is the most effective procedure among various studies that were designed for the same purpose.[12,32]

After numerous experimental studies, clinical application of ghrelin commenced in healthy volunteers and then extended to patients with heart failure,[23] pulmonary disease,[24] and cancer cachexia.[25] The results of these studies confirmed the safety of ghrelin administration. In our study, the patients in the 2 groups showed no differences in postoperative complications (eg, infections, delayed wound healing, thromboembolism) and length of hospital stay. However, 1 of the 11 patients developed diaphoresis, corresponding to National Cancer Institute Common Terminology Criteria for Adverse Events grade 1. Although we stopped ghrelin administration following the study protocol, this symptom was consistently reported in previous trials although it was tolerated by patients.[23-25,29] The overall positive effects of ghrelin such as body weight gain and increase in food intake calories were observed consistently in all clinical trials, including the present study.[21-25] In addition, improvement of disease-specific status has been reported, including patients with chronic heart failure[23] and those with chronic obstructive pulmonary disease.[24]

To our knowledge, the present study is the first clinical trial in the field of gastroenterological surgery. Moreover, the present study differs in 2 aspects from previous studies.[23-25] The first difference related to the study subjects; the subjects enrolled in previous clinical studies were cachexic emaciated patients in whom the level of circulating ghrelin was predicted to rise. It has been considered that the efficacy of exogenous ghrelin is limited because of down-regulation by high endogenous ghrelin. In contrast, in the present study, in which circulating ghrelin levels were extremely low due to total gastrectomy, we replaced the low levels of endogenous ghrelin with an exogenous one; therefore, it seems more physiologically related to study the effect of ghrelin administration. Another point is that complete vagotomy at the esophagogastric junction was performed during total gastrectomy in our patients. Because the vagus nerve mediates both efferent and afferent ghrelin signals,[33-35] it was suspected that exogenous ghrelin would not adequately interact in the hypothalamus. In animal experiments, vagotomy or chemical blockade of the vagal

signal abolished the effects of intravenously administrated ghrelin.[36] In vagotomized patients, ghrelin administration did not increase food intake.[37] However, other studies reported that ghrelin administered intraperitoneally successfully stimulated food intake after vagotomy in rats[38] and that ghrelin administration in vagotomized patients enhanced GH secretion.[39] These animal experiments and clinical studies indicate that the effects of ghrelin administration are still controversial, at least in vagotomized patients. In the present study, intravenous administration of exogenous ghrelin successfully stimulated food intake and appetite immediately after total gastrectomy. Our results suggest that the administered ghrelin crossed the blood-brain barrier to the central nervous system, probably increasing the appetite signal through not only the vagal pathway but also the circulation. The relationship between ghrelin and vagotomy remains poorly defined, and further studies should be performed in the future.

BMR accounts for between 60% and 70% of the total energy expenditure in adults.[40] Furthermore, the fat-free mass is considered the best single predictor of energy expenditure, and 53% to 88% of the variation in BMR is accounted for by fat-free mass.[41] In the placebo group, the BMR decreased significantly after total gastrectomy, whereas it did not change in the ghrelin group. This result was consistent with the significant decrease in lean body mass, which was limited to the placebo group. In animal experiments, ghrelin enhances abdominal fat storage in white adipose tissue in rats,[19] whereas clinical studies, including the present study, have shown that ghrelin increases lean body mass relative to fat mass.[23,24] Differences in species and patient status may influence the effect of ghrelin administration on fat metabolism. Preservation of lean body mass against the postoperative catabolic metabolism might be caused by ghrelin-stimulated GH secretion from the pituitary gland. However, serum GH levels were stable in the 2 groups, probably due to the rapid turnover of GH. This phenomenon was already reported in a previous phase I study.[29] Baseline leptin levels tended to be lower in the ghrelin group, probably because this group included more men, who generally have lower leptin levels than women.[42,43] Leptin levels significantly decreased in parallel with the decrease in fat mass in both the ghrelin and placebo groups.

The influence of cancer proliferation is another issue of safety in ghrelin studies. Several in vitro studies reported the expression of ghrelin receptor in cancer cells and that ghrelin weakly enhanced their proliferation, for example, in prostate[44] and pancreatic[45] cancer cells. However, another study reported that ghrelin inhibited proliferation and increased apoptosis in a lung cancer cell line.[46] In a preliminary experiment in our laboratory using various gastric cancer cell lines, all cells examined were negative for ghrelin receptor and showed no growth response to exogenous ghrelin (unpublished observation, March 2005). In clinical studies of cancer cachexic patients, no adverse events concerning tumor growth stimulation have been reported.[25] With respect to the present clinical trial, this argument was partly evaded because patients who met the inclusion criteria accounted for more than 90% curability by surgery alone[31] and ghrelin was administered for only 10 days. However, care should be taken when administering ghrelin over longer periods.

Although we successfully demonstrated a short-term effect of ghrelin administration on food intake, appetite, body weight, and other parameters, its long-term effect and benefit still need to be evaluated before clinical application. Because ghrelin secretion does not recover even several years after total gastrectomy, long-term administration of ghrelin is probably required to maintain the short-term effects. For this purpose, ghrelin poses a practical problem in that it is an unstable short-acting peptide and needs to be administered intravenously. An easier administration route, such as subcutaneous injection and inhalation, should be investigated to allow outpatient and home use. GH secretagogues, which were discovered before ghrelin, are orally available and perhaps could be used as ghrelin substitutes. For example, RC-1291 is orally available, well tolerated, and effective in promoting body weight gain, as demonstrated in a phase I study in healthy volunteers.[47] Another issue worth further investigation is the clinical benefits of ghrelin therapy, because it is argued that increases in appetite and body weight are not sufficient reasons for medication. Thus, further studies are needed to evaluate other aspects of ghrelin administration, such as reduction of total medical cost and hospital admission, improvement of social activity and quality of life, and postoperative survival. For example, postoperative body weight loss is most progressive and rehabilitation is most important in the first 3 months after surgery. It is possible that ghrelin administration for at least 3 months would improve postoperative recovery.

In conclusion, this prospective randomized study in a limited number of patients provides convincing data for the beneficial effects of ghrelin on body weight and dietary activity after total gastrectomy. Although there are some issues to be resolved before clinical application, including drug delivery system, duration of administration, and adequate assessment of clinical benefits, surgeons dealing with gastric cancers and other gastroesophageal diseases should be encouraged by the availability of ghrelin. Because surgery is essentially not physiologic and highly invasive for the body but the most reliable therapeutic option to cure cancer, it is our obligation to invent novel procedures to minimize its side effects.

References

1. Demas GE, Drazen DL, Nelson RJ, et al. Reductions in total body fat decrease humoral immunity. Proc Roy Soc B-Biol Sci 2003; 270:905–911.
2. Marinho LA, Rettori O, Vieira-Matos AN, et al. Body weight loss as an indicator of breast cancer recurrence. Acta Oncol 2001;40: 832–837.
3. Tsugane S, Sasaki S, Tsubono Y. Under- and overweight impact on mortality among middle-aged Japanese men and women: a 10-y follow-up of JPHC Study cohort I. Int J Obes Relat Metab Disord 2002:529–537.
4. Bae JM, Park JW, Yang HK, et al. Nutritional status of gastric cancer patients after total gastrectomy. World J Surg 1998;22: 254–260.
5. Friess H, Bohm J, Muller MW, et al. Maldigestion after total gastrectomy is associated with pancreatic insufficiency. Am J Gastroenterol 1996;91:341–347.
6. Melissas J, Kampitakis E, Schoretsanitis G, et al. Does reduction in gastric acid secretion in bariatric surgery increase diet-induced thermogenesis? Obes Surg 2002;12:399–403.
7. Adachi S, Takeda T, Fukao K. Evaluation of esophageal bile reflux after total gastrectomy by gastrointestinal and hepatobiliary dual scintigraphy. Surg Today 1999;29:301–306.
8. Armbrecht U, Lundell L, Stockbruegger RW. Nutrient malassimilation after total gastrectomy and possible intervention. Digestion 1987;37:56–60.
9. Iesato H, Ohya T, Ohwada S, et al. Jejunal pouch interposition with an antiperistaltic conduit as a pyloric ring substitute after standard distal gastrectomy: a comparison with the use of an isoperistaltic conduit. Hepatogastroenterology 2000;47:756–760.
10. Braga M, Zuliani W, Foppa L, et al. Food intake and nutritional status after total gastrectomy: results of a nutritional follow-up. Br J Surg 1998;75:477–480.
11. Bergh C, Sjostedt S, Hellers G, et al. Meal size, satiety and cholecystokinin in gastrectomized humans. Physiol Behav 2003; 78:143–147.
12. Fein M, Fuchs KH, Thalheimer A, et al. Long-term benefits of Roux-en-Y pouch reconstruction after total gastrectomy: a randomized trial. Ann Surg 2008;247:759–765.
13. Liedman B. Symptoms after total gastrectomy on food intake, body composition, bone metabolism, and quality of life in gastric cancer patients: is reconstruction with a reservoir worthwhile? Nutrition 1999;15:677–682.
14. Kojima M, Hosoda H, Date Y, et al. Ghrelin is a growth-hormone-releasing acylated peptide from stomach. Nature 1999;402: 656–660.
15. Date Y, Kojima M, Nakazato M, et al. Ghrelin, a novel growth hormone-releasing acylated peptide, is synthesized in a distinct endocrine cell type in the gastrointestinal tracts of rats and humans. Endocrinology 2000;141:4255–4260.
16. Leite-Moreira AF, Soares JB. Physiological, pathological and potential therapeutic roles of ghrelin. Drug Discov Today 2007;12: 276–288.
17. Shintani M, Ogawa Y, Ebihara K, et al. Ghrelin, an endogenous growth hormone secretagogue, is a novel orexigenic peptide that antagonizes leptin action through the activation of hypothalamic neuropeptide Y/Y1 receptor pathway. Diabetes 2001;50:227–232.
18. Masuda Y, Tanaka T, Inomata N, et al. Ghrelin stimulates gastric acid secretion and motility in rats. Biochem Biophys Res Commun 2000;276:905–908.
19. Davies JS, Kotokorpi P, Eccles SR, et al. Ghrelin induces abdominal obesity via GHS-R-dependent lipid retention. Mol Endocrinol 2009;23:914–924.
20. Wu R, Dong W, Zhou M, et al. Ghrelin attenuates sepsis-induced acute lung injury and mortality in rats. Am J Respir Crit Care Med 2007;176:805–813.
21. Wren AM, Seal LJ, Cohen MA, et al. Ghrelin enhances appetite and increases food intake in human. J Clin Endocrinol Metab 2001;86:5992–5995.
22. Neary NM, Small CJ, Wren AM, et al. Ghrelin increases energy intake in cancer patients with impaired appetite: acute, randomized, placebo-controlled trial. J Clin Endocrinol Metab 2004;89: 2832–2836.
23. Nagaya N, Moriya J, Kangawa K, et al. Effects of ghrelin administration on left ventricular function, exercise capacity, and muscle wasting in patients with chronic heart failure. Circulation 2004;110:3674–3679.
24. Nagaya N, Itoh T, Kangawa K, et al. Treatment of cachexia with ghrelin in patients with COPD. Chest 2005;128:1187–1193.
25. Strasser F, Lutz TA, Maeder MT, et al. Safety, tolerability and pharmacokinetics of intravenous ghrelin for cancer-related anorexia/cachexia: a randomised, placebo-controlled, double-blind, double-crossover study. Br J Cancer 2008;98:300–308.
26. Karamanakos SN, Vagenas K, Kalfarentzos F, et al. Weight loss, appetite suppression, and changes in fasting and postprandial ghrelin and peptide-YY levels after Roux-en-Y gastric bypass and sleeve gastrectomy: a prospective, double blind study. Ann Surg 2008;247:401–407.
27. Takachi K, Doki Y, Ishikawa O, et al. Postoperative ghrelin levels and delayed recovery from body weight loss after distal or total gastrectomy. J Surg Res 2006;130:1–7.
28. Doki Y, Takachi K, Ishikawa O, et al. Ghrelin reduction after esophageal substitution and its correlation to postoperative body weight loss in esophageal cancer patients. Surgery 2006;139: 797–805.
29. Akamizu T, Takaya K, Kangawa K, et al. Pharmacokinetics, safety, and endocrine and appetite effects of ghrelin administration in young healthy subjects. Eur J Endocrinol 2004;150:447–455.
30. Shiraishi N, Yasuda K, Kitano S. Laparoscopic gastrectomy with lymph node dissection for gastric cancer. Gastric Cancer 2006; 9:167–176.
31. Nomura S, Kaminishi M. Surgical treatment of early gastric cancer. Dig Surg 2007;24:96–100.
32. Lehnert T, Buhl K. Techniques of reconstruction after total gastrectomy for cancer. Br J Surg 2004;91:528–539.
33. Asakawa A, Inui A, Kaga T, et al. Ghrelin is an appetite-stimulatory signal from stomach with structural resemblance to motilin. Gastroenterology 2001;120:337–345.
34. Sato N, Kanai S, Takano S, et al. Central administration of ghrelin stimulates pancreatic exocrine secretion via the vagus in conscious rats. Jpn J Physiol 2003;53:443–449.
35. Simonian HP, Kresge KM, Boden GH, et al. Differential effects of sham feeding and meal ingestion on ghrelin and pancreatic polypeptide levels: evidence for vagal efferent stimulation mediating ghrelin release. Neurogastroenterol Motil 2005;17:348–354.
36. Date Y, Murakami N, Nakazato M, et al. The role of the gastric afferent vagal nerve in ghrelin-induced feeding and growth hormone secretion in rats. Gastroenterology 2002;123:1120–1128.
37. le Roux CW, Neary NM, Halsey TJ, et al. Ghrelin does not stimulate food intake in patients with surgical procedures involving vagotomy. J Clin Endocrinol Metab 2005;90:4521–4524.
38. Arnold M, Mura A, Langhans W, et al. Gut vagal afferents are not necessary for the eating-stimulatory effect of intraperitoneally injected ghrelin in the rat. J Neurosci 2006;26:11052–11060.
39. Takeno R, Okimura Y, Iguchi G, et al. Intravenous administration of ghrelin stimulates growth hormone secretion in vagotomized

patients as well as normal subjects. Eur J Endocrinol 2004;151:447–450.
40. Shetty P. Energy requirements of adults. Public Health Nutr 2005;8:994–1009.
41. Nelson KM, Weinsier RL, Long CL, et al. Prediction of resting energy expenditure from fat-free mass and fat mass. Am J Clin Nutr 1992;56:848–856.
42. Kennedy A, Gettys TW, Watson P, et al. The metabolic significance of leptin in humans: gender-based differences in relationship to adiposity, insulin sensitivity, and energy expenditure. J Clin Endocrinol Metab 1997;82:1293–1300.
43. Ostlund RE Jr, Yang JW, Klein S, et al. Relation between plasma leptin concentration and body fat, gender, diet, age, and metabolic covariates. J Clin Endocrinol Metab 1996;81:3909–3913.
44. Yeh AH, Jeffery PL, Duncan RP, et al. Ghrelin and a novel preproghrelin isoform are highly expressed in prostate cancer and ghrelin activates mitogen-activated protein kinase in prostate cancer. Clin Cancer Res 2005;11:8295–8303.
45. Duxbury MS, Waseem T, Ito H, et al. Ghrelin promotes pancreatic adenocarcinoma cellular proliferation and invasiveness. Biochem Biophys Res Commun 2003;309:464–468.
46. Cassoni P, Allia E, Marrocco T, et al. Ghrelin and cortistatin in lung cancer: expression of peptides and related receptors in human primary tumors and in vitro effect on the H345 small cell carcinoma cell line. J Endocrinol Invest 2006;29:781–790.
47. Garcia JM, Polvino WJ. Effect on body weight and safety of RC-1291, a novel, orally available ghrelin mimetic and growth hormone secretagogue: results of a phase I, randomized, placebo-controlled, multiple-dose study in healthy volunteers. Oncologist 2007;12:594–600.

Received July 20, 2009. Accepted December 17, 2009.

Reprint requests

Address requests for reprints to: Shuji Takiguchi, MD, PhD, Department of Gastroenterological Surgery, Osaka University Graduate School of Medicine, 2-2 Suita City Yamadaoka, Osaka, Japan. e-mail: stakiguchi@gesurg.med.osaka-u.ac.jp; fax: (81) 6-6879-3259.

Acknowledgments

Online registry: http://www.umin.ac.jp; clinical trial no. UMIN000001925.

The authors thank Tomoyuki Sugimoto from the Department of Biomedical Statistics, Osaka University, for the advice on statistical analysis as well as the nutritional management room staff of Osaka University Hospital for calculating food intake calories per day in this study.

Conflicts of interest

The authors disclose no conflicts.

Ann Surg Oncol (2010) 17:967–972
DOI 10.1245/s10434-009-0865-y

Annals of
SURGICAL ONCOLOGY
OFFICIAL JOURNAL OF THE SOCIETY OF SURGICAL ONCOLOGY

ORIGINAL ARTICLE – COLORECTAL CANCER

TGM2 Is a Novel Marker for Prognosis and Therapeutic Target in Colorectal Cancer

Norikatsu Miyoshi, MD[1], Hideshi Ishii, MD[1,2], Koshi Mimori, MD[2], Fumiaki Tanaka, MD[2], Toshiki Hitora, MD[1], Mitsuyoshi Tei, MD[1], Mitsugu Sekimoto, MD[1], Yuichiro Doki, MD, PhD[1], and Masaki Mori, MD, PhD, FACS[1]

[1]Department of Gastroenterological Surgery, Osaka University Graduate School of Medicine, Osaka, Japan; [2]Division of Molecular and Surgical Oncology, Department of Molecular and Cellular Biology, Medical Institute of Bioregulation, Kyushu University, Ohita, Japan

ABSTRACT

Background. Transglutaminase 2 (*TGM2*) plays a role in cell growth and survival through the antiapoptosis signaling pathway.

Methods. We analyzed *TGM2* gene expression in 91 paired cases of colorectal cancer (CRC) and noncancerous regions and seven CRC cell lines to demonstrate the importance of *TGM2* expression for the prediction of prognosis of CRC. *TGM2* expression was higher in CRC tissue than in corresponding normal tissue by real-time reverse transcriptase–polymerase chain reaction ($P = .015$).

Results. Patients in the high *TGM2* expression group showed a poorer overall survival rate than those in the low expression group ($P = .001$), indicating that the increase in *TGM2* expression was an independent prognostic factor. *TGM2* was also expressed in the seven CRC cell lines. The in vitro proliferation assay showed that *TGM2* expression is involved with tumor growth.

Conclusions. The present study suggests that *TGM2* is useful as a predictive marker for patient prognosis and may be a novel therapeutic target for CRC.

Cancer is a major public health problem in developed countries, while the incidence of colorectal cancer (CRC) has greatly increased in Japan in recent years as a result of lifestyle changes.[1] CRC is now one of the most important causes of death from neoplastic disease in Japan.[1] Therefore, identification of the genes responsible for the development and progression of CRC and understanding the clinical significance are critical for the diagnosis and adequate treatment of the disease.

Transglutaminase 2, *TGM2*, is a family of enzymes that catalyzes the formation of an amide bond between the γ-carboxamide groups of peptide-bound glutamine residues and the primary amino groups in various compounds.[2,3] Several studies have reported that that increased expression of *TGM2* indicates prolonged cell survival and the prevention of apoptosis.[4–9]

We analyzed *TGM2* in seven human gastrointestinal cancer cell lines and 91 paired cases of CRC and noncancerous regions to identify the importance of *TGM2* expression for prognosis and to suggest that it be a candidate novel marker for the prognosis with functional relevance in CRCs.

MATERIALS AND METHODS

Clinical Tissue Samples

From 1992 to 2002, 91 patients (62 men, 29 women) with CRC underwent surgery at the Medical Institute of Bioregulation at Kyusyu University. Primary CRC specimens and adjacent normal colorectal mucosa were obtained from patients after receiving informed consent in accordance with the institutional guidelines. Every patient was definitively identified with CRC on the basis of clinicopathological findings. Tissues were extracted immediately after surgical resections. The specimens were immediately fixed in formalin, processed through graded ethanol,

Electronic supplementary material The online version of this article (doi:10.1245/s10434-009-0865-y) contains supplementary material, which is available to authorized users.

First Received: 20 July 2009;
Published Online: 22 December 2009

M. Mori, MD, PhD, FACS
e-mail: mmori@gesurg.med.osaka-u.ac.jp